A potassium-dependent oxygen sensing pathway regulates plant root hydraulics

Zaigham Shahzad, Matthieu Canut, Colette Tournaire-Roux, Alexandre Martiniere, Yann Boursiac, Olivier Loudet, Christophe Maurel

Article

Cell

A Potassium-Dependent Oxygen Sensing Pathway Regulates Plant Root Hydraulics

Graphical Abstract

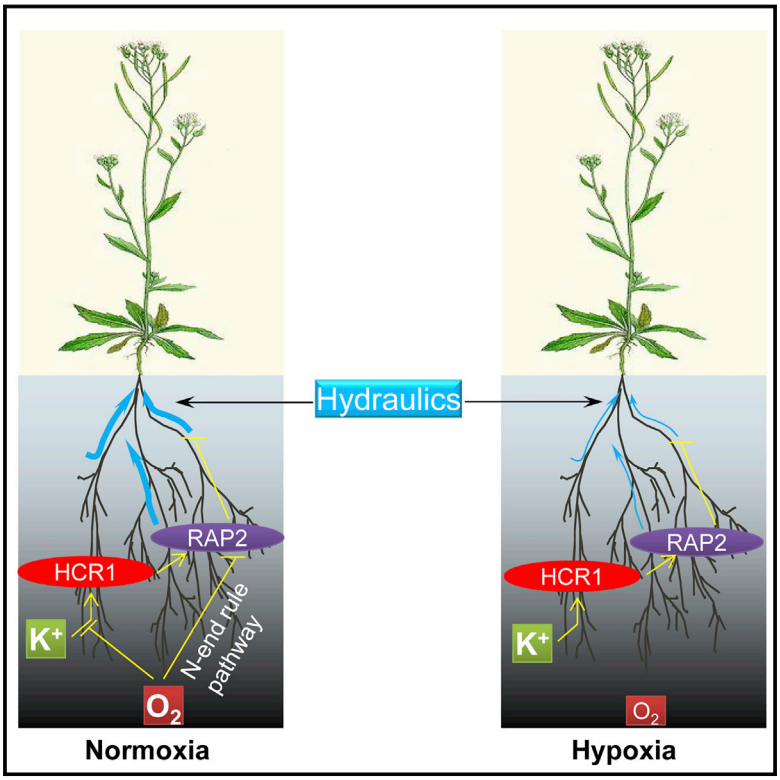

Authors

Zaigham Shahzad, Matthieu Canut, Colette Tournaire-Roux, Alexandre Martinière, Yann Boursiac, Olivier Loudet, Christophe Maurel

Correspondence

christophe.maurel@supagro.inra.fr

In Brief

A pathway that integrates oxygen and potassium levels to modulate root hydraulics allows plants to survive flooding.

Highlights

- Natural variants of *HCR1* control root hydraulic conductivity (Lp_r) in *Arabidopsis*
- *HCR1* is regulated by O_2 supply in a K^+-dependent manner
- *HCR1* integrates O_2 and K^+ signaling to regulate Lp_r and anaerobic gene expression
- *HCR1* regulates the abundance of RAP2.12 transcription factor to downregulate Lp_r

Data Resource

GSE78087

Shahzad et al., 2016, Cell *167*, 1–12
September 22, 2016
http://dx.doi.org/10.1016/j.cell.2016.08.068

Article

Cell

A Potassium-Dependent Oxygen Sensing Pathway Regulates Plant Root Hydraulics

Zaigham Shahzad,[1] Matthieu Canut,[2] Colette Tournaire-Roux,[1] Alexandre Martinière,[1] Yann Boursiac,[1] Olivier Loudet,[2] and Christophe Maurel[1,3,*]

[1]Biochimie et Physiologie Moléculaire des Plantes, UMR5004, INRA/CNRS/Montpellier SupAgro/Université Montpellier, 34060 Montpellier, France

[2]Institut Jean-Pierre Bourgin, INRA/AgroParisTech/CNRS/Université Paris-Saclay, RD10, 78026 Versailles Cedex, France

[3]Lead Contact

*Correspondence: christophe.maurel@supagro.inra.fr

http://dx.doi.org/10.1016/j.cell.2016.08.068

SUMMARY

Aerobic organisms survive low oxygen (O_2) through activation of diverse molecular, metabolic, and physiological responses. In most plants, root water permeability (in other words, hydraulic conductivity, Lp_r) is downregulated under O_2 deficiency. Here, we used a quantitative genetics approach in *Arabidopsis* to clone *Hydraulic Conductivity of Root 1* (*HCR1*), a Raf-like MAPKKK that negatively controls Lp_r. HCR1 accumulates and is functional under combined O_2 limitation and potassium (K^+) sufficiency. HCR1 regulates Lp_r and hypoxia responsive genes, through the control of RAP2.12, a key transcriptional regulator of the core anaerobic response. A substantial variation of HCR1 in regulating Lp_r is observed at the *Arabidopsis* species level. Thus, by combinatorially integrating two soil signals, K^+ and O_2 availability, HCR1 modulates the resilience of plants to multiple flooding scenarios.

INTRODUCTION

The growth and survival of land plants critically depend on efficient soil water uptake. To achieve this, higher plants have evolved highly specialized root systems. While their sustained growth and branching allow optimal soil exploration, water permeability of roots (in other words, root hydraulic conductivity, Lp_r) favors the radial transfer of water from the soil into the root stele for subsequent transport to the shoot. Aquaporins, water channel proteins that facilitate water transport across root cell membranes (Maurel et al., 2015), are main effectors of radial water transport. They mediate the adjustment of root hydraulics in response to plant hormones or multiple edaphic or climatic factors (Aroca et al., 2012; Maurel et al., 2015), thereby contributing to maintenance of the plant water status under changing environmental conditions. Although they represent a key point for adaptation of wild plant species to diverse natural habitats and a major target for crop improvement, the signaling mechanisms that link soil properties to root hydraulics and aquaporin functions remain largely unknown. The lack of proper direct genetic screens using plant hydraulics as a trait has restricted advances in this field.

Oxygen (O_2), which supports respiratory energy production, is, besides water, another critical factor for plant performance. Yet, its availability can be reduced by flooding or soil compaction. Eukaryotic organisms survive limited O_2 availability (hypoxia) by reprograming gene expression and producing energy through ethanolic fermentation (Gibbs et al., 2015; Tadege et al., 1999). Primary activation of hypoxia signaling is achieved by *Hypoxia Inducible Factor-1* (*HIF-1*) transcription factors (TFs) in animals and ethylene-responsive factor group VII (ERF-VII) TFs in plants. The model plant species *Arabidopsis thaliana* possesses five ERF-VII TFs named Related to AP (RAP) 2.2, RAP2.3, RAP2.12, Hypoxia Responsive ERF (HRE) 1, and HRE2 (Nakano et al., 2006). Whereas *HRE1* and *HRE2* are regulated in an O_2-dependent manner at both transcriptional and post-transcriptional levels (Gibbs et al., 2011; Licausi et al., 2010), *RAP2.12* is mostly regulated at post-transcriptional level (Licausi et al., 2010, 2011). Under non-limiting O_2 concentrations (normoxia), *Arabidopsis* ERF-VII proteins including RAP2.12 are oxidized and degraded via an evolutionary conserved N-end rule pathway. Conversely, their stabilization under hypoxia triggers anaerobic gene expression. However, additional, largely unknown posttranslational mechanisms are thought to contribute to the regulation of ERF-VII TFs (Gibbs et al., 2015). Early adaptive responses of plants to O_2 deficiency also include adjustments of their water and nutritional status. For instance, hypoxia caused by flooding can lead to downregulation of Lp_r, leaf dehydration, and stomatal closure (Aroca et al., 2012). In *Arabidopsis*, the early root hydraulic response to hypoxia is caused by pH-dependent gating of Plasma membrane Intrinsic Proteins (PIPs) aquaporins (Tournaire-Roux et al., 2003). Uptake and partitioning of macronutrients such as nitrogen, phosphate, or potassium (K^+) is also inhibited in plants during hypoxia (Shabala et al., 2014; Wiengweera and Greenway, 2004), possibly due to reduced cell energy status. In addition, each of these macronutrients exerts contrasting effects on Lp_r through regulation of aquaporins (Maurel et al., 2015). However, it is not known how plant roots can handle multiple soil signals simultaneously. In particular, cross-talks of hypoxia with other abiotic stresses and the impact of such integrated signaling on plant adaptation to low-O_2 have not been explored.

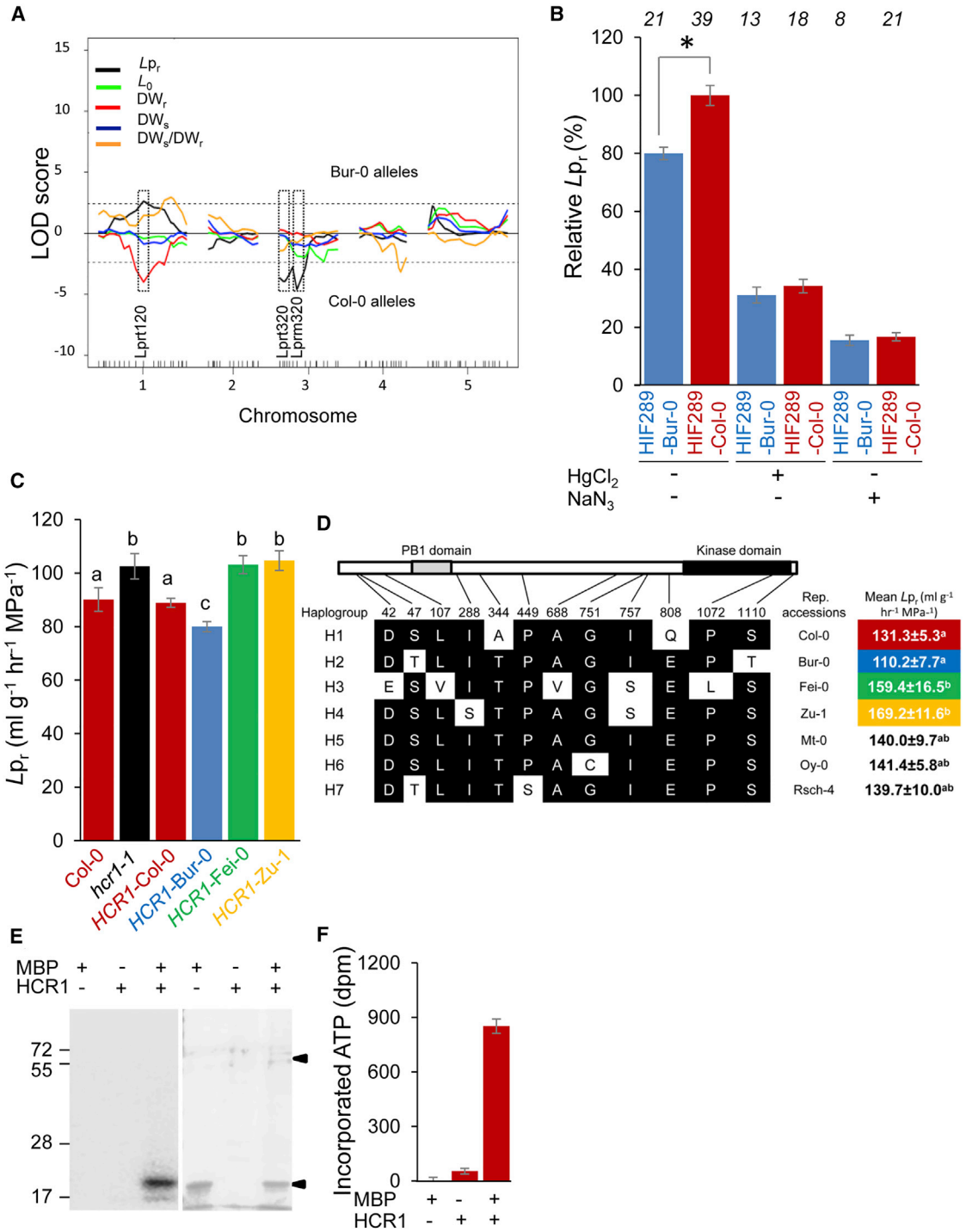

Figure 1. Natural Variation of *HCR1* in *Arabidopsis*

(A) QTL map for hydraulic (Lp_r; root hydraulic conductance: L_o) and growth (root dry weight: DW_r; shoot dry weight: DW_s; DW_r-to-DW_s ratio: DW_r/DW_s) traits in an *Arabidopsis* RIL population derived from a cross between Bur-0 and Col-0. Positive and negative LOD scores correspond to positive contribution of Bur-0 and Col-0 parental alleles, respectively. LOD significance threshold of 2.5 was obtained from permutation. Three significant Lp_r QTLs are indicated using dotted rectangles.

(B) Average Lp_r (±SE) of HIF289 fixed for Bur-0 (blue) or Col-0 (red) allele of Lprm320, before and after treatment with $HgCl_2$ or NaN_3. Data from the indicated number of plants in two to four independent experiments.

(C) Cloning of Lprm320. Mean Lp_r (±SE) is shown for Col-0, *hcr1-1*, and *hcr1-1* plants expressing a similar *HCR1* genomic region from Col-0, Bur-0, Fei-0, or Zu-1 (n = 16–125, N = 3). Two to five independent transgenic lines were phenotyped for each allele. See also Figures S1A–S1D and S2A–S2C.

(legend continued on next page)

To identify genetic factors relevant to the regulation of root water transport and plant adaptation to natural habitats, we explored the variation of Lp_r in wild isolates (accessions) of *Arabidopsis*. Multiple quantitative trait loci (QTLs) controlling Lp_r were detected in a recombinant population obtained from a cross between two accessions. Positional cloning of *Hydraulic Conductivity of Root 1* (*HCR1*), one of these Lp_r QTL genes, revealed a Raf-like MAPKKK (Rapidly accelerated fibrosarcoma-like mitogen activated protein kinase kinase kinase) that negatively regulates root water transport in response to both K^+ and O_2 availability. Furthermore, we show that *HCR1* controls a general K^+-dependent molecular pathway for hypoxia signaling in plants. Thus, *HCR1* links root hydraulics and whole-genome transcriptional responses to two fundamental soil parameters. We propose that its natural variations underlie distinct plant strategies for plant growth under O_2-limiting conditions.

RESULTS

Fine Mapping of a Lp_r QTL in *Arabidopsis*

We previously showed that the Col-0 and Bur-0 accessions have distinct root hydraulic profiles, the latter showing a relatively low contribution of aquaporins to Lp_r (Sutka et al., 2011). Here, we used a set of 123 recombinant inbred lines (RILs) obtained from a cross between these accessions and performed QTL mapping for Lp_r. The RILs were also phenotyped for plant growth, to check for possible pleiotropic effects on plant hydraulics. Although all investigated traits are highly sensitive to environment, standardized plant growth and hydraulic phenotyping procedures yielded broad-sense heritabilities (h^2) $\geq$0.45 (Table S1). Three QTLs for Lp_r named Lprm120, Lprt320, and Lprm320 were detected on chromosomes 1, 3, and 3, respectively (Figure 1A; Table S2). Lprm320 explains 15% of total phenotypic variance (Table S2), does not co-localize with growth related QTLs (Figure 1A), and was selected for further studies. Its effects were confirmed using Nearly Isogenic Lines (NILs) of Heterogeneous Inbred Family (HIF)-type fixed for either Bur-0 or Col-0 allele. HIF289, which is heterozygous for a >4.2-Mb region encompassing Lprm320, recapitulated the positive versus negative effects of Col-0 and Bur-0 alleles on Lp_r, with a 19.2% ± 2% difference between genotypes (Figure 1B; Table S2). After treatment with mercuric chloride (50 μM $HgCl_2$; 40 min) or sodium azide (1 mM NaN_3; 30 min), two pharmacological agents inhibiting root aquaporins through independent modes of action (Sutka et al., 2011), the alternative genotypes of HIF289 exhibited similar, strongly reduced Lp_r, indicating that their distinct Lp_r under standard conditions are due to differences in aquaporin activity (Figure 1B). To restrain the QTL region, fine mapping was performed using recombinant HIFs (rHIFs) generated by selfing HIF289 and selecting progeny lines with recombination break points at different intervals (Figure S1A). In total, 16 rHIFs were tested for segregation of Lp_r. Extensive characterization of two genotypically close rHIFs (289-40 and 289-57) that showed differential segregation for Lp_r helped restrain the QTL region to ~15 kb.

HCR1, a Gene that Negatively Controls Lp_r at the Species-wide Level

The candidate interval harbored five open reading frames (Figure S1A). Phenotyping of knockout mutant lines of each of these (Key Resources Table) revealed that only two independent mutants of At3g24715 exhibited altered Lp_r (>15% increase) as compared to Col-0 (Figure S1B), while no alteration in root growth (dry weight) was observed (Figure S1C). Moreover, $HgCl_2$ and NaN_3 inhibition experiments indicated that the difference in Lp_r between Col-0 and At3g24715 mutants can be accounted for by a difference in aquaporin activity (Figure S1D). Because of such consistent root water transport phenotypes in two independent allelic knockout mutants, At3g24715 was named *Hydraulic Conductivity of Root 1* (*HCR1*). To confirm that *HCR1* is the gene underlying Lprm320, we first performed a quantitative complementation of the Lp_r phenotype of one of knockout mutants (*hcr1-2*) in a cross with advanced rHIFs bringing either a Bur-0 or a Col-0 allele. The latter conferred on *hcr1-2* a higher Lp_r than the former, whereas the two alleles had indistinguishable effects in a cross with Col-0 (Figure S2A). Such an interaction between the QTL allele and mutant background is a strong indication that variation at *HCR1* is responsible for Lprm320. Further, molecular complementation of the other knockout mutant (*hcr1-1*) was performed by introduction of genomic Bur-0 and Col-0 alleles through *Agrobacterium*-mediated transformation. *HCR1* mRNA abundance was analyzed using qRT-PCR in independent transgenic lines to confirm the expression of transgenes (Figure S2B). The two alleles reduced the Lp_r of *hcr1-1*, independent of their expression level, but with distinct amplitude (Col-0: −13.3% ± 3.0%; Bur-0: −22.0% ± 2.8%) consistent with the QTL effects (Figures 1C and S2C). The overall data establish that *HCR1* underlies Lprm320 and acts as a negative regulator of Lp_r.

HCR1 belongs to the B4 group of Raf-like MAPKKKs (Ichimaru and MAPK group, 2002) with seven uncharacterized members in *Arabidopsis*. HCR1 harbors in its N-terminal region a Phox/Bem1p (PB1) domain for putative protein-protein interaction, and in its C-terminal region a protein kinase domain sharing similarity with Raf kinases (Figure 1D). Following discovery of *HCR1* based on genetic differences between two wild accessions, we further characterized its natural variations. A worldwide collection of 72 *Arabidopsis* accessions (Table S3) could be classified into seven haplogroups (H1–H7), according to polymorphisms in HCR1 predicted protein sequence (Figure 1D). All accessions were phenotyped for Lp_r, with average values showing significant differences between some haplogroups.

(D) Schematic representation of HCR1 protein structure. Amino acid polymorphism in *Arabidopsis* HCR1 haplogroups (H1–H7 defined by representative accessions) are projected on the structure. Mean Lp_r ± SE (n = 6–15 independent accessions) within each haplogroup is shown.
(E and F) In vitro phosphorylation of MBP by recombinant kinase domain of HCR1 ($HCR1_{801–1117}$). Phosphorylated MBP was detected by autoradiography (E) or quantified by spotting on phosphocellulose filters (means ± SE) (F). Right panel in (E) shows corresponding Coomassie blue stained gel as protein loading control. Arrow heads indicate bands corresponding to MBP, and $HCR1_{801–1117}$ (see also Figure S2D).
See also Figures S1 and S2.

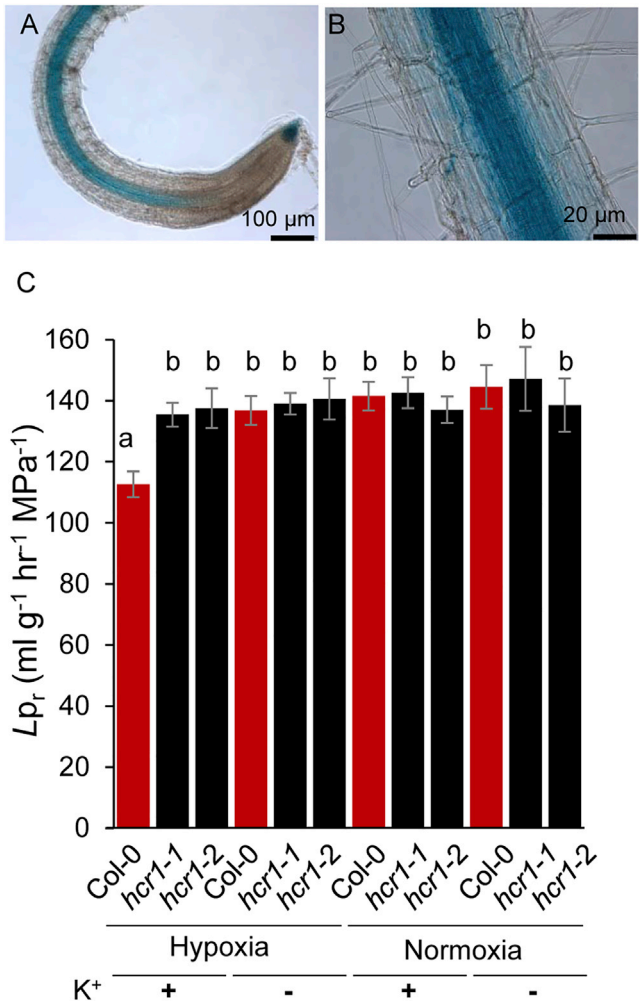

Figure 2. *HCR1* Is a Root-Expressed Protein Kinase that Regulates Lp_r under K^+-Replete O_2-Deficient Conditions

(A and B) prom*HCR1*::GUS expression was detected in the root stele (A and B) and root tip (A) (see also Figures S3A–S3C).

(C) Lp_r of Col-0 and *hcr1* plants grown under standard (hypoxia) or normoxia conditions in the presence or absence of K^+ (means ± SE, n ≥ 11, N = 3). For K^+-depleted conditions, 19-day-old plants were transferred to a solution lacking K^+ for 2 days prior to Lp_r measurements (see also Figures S3D and S3E).

See also Figure S3.

Notably, H3 and H4 exhibited higher Lp_r than H1 and H2, which comprise Col-0 and Bur-0, respectively. We chose Fei-0 and Zu-1 as representative accessions for haplogroups H3 and H4, respectively, and introduced their corresponding *HCR1* genomic regions into *hcr1-1*. These transformations led to proper expression of the two *HCR1* allelic forms (Figure S2B) but did not alter *hcr1-1* for Lp_r (Figures 1C and S2C), indicating that they are inactive in a Col-0 background. Thus, natural *HCR1* forms fall in at least three functional groups and contribute to Lp_r variation at the species-wide level.

The enzymatic activity of the C-terminal kinase domain of Col-0 HCR1 ($HCR1_{821–1117}$) was investigated using a fusion with glutathione S-transferase (GST) and production from an *Escherichia coli* expression system. The generic substrate Myelin Basic Protein (MBP) could be phosphorylated in vitro by the recombinant protein (Figures 1E and 1F). Regarding the functional significance of polymorphisms among HCR1 haplogroups, we found that, in contrast to its Col-0, Bur-0, and Zu-1 counterparts, a HCR1 fragment ($HCR1_{801–1117}$) encompassing the protein kinase domain and prepared from Fei-0 could not phosphorylate MBP (Figure S2D). This defect is related to the specific Pro-to-Leu substitution at position 1072 in the protein kinase domain of the Fei-0 form. It is consistent with the inability of the Fei-0 allele to complement the *hcr1-1* mutant in a Col-0 background.

HCR1 Regulates Lp_r under K^+-Replete O_2-Deficient Conditions

Because it is a reference accession in *Arabidopsis* studies, the parental line Col-0 was selected for further functional characterization of *HCR1*. Transgenic expression of a prom*HCR1*::β-glucuronidase (GUS) chimeric gene indicated a preferential promoter activity in the root stele, consistent with a general role in root hydraulics (Figures 2A and 2B). Reporter gene expression was not detectable in leaves and plant reproductive parts (Figures S3A–S3C). The Raf-like MAPKKK structure of HCR1 is suggestive of a signaling function. We therefore hypothesized a role for *HCR1* in Lp_r response to some of endogenous or environmental cues acting in roots and present in our standard growth conditions. To investigate these, Col-0 and *hcr1* plants were comparatively phenotyped for Lp_r using various hormonal or abiotic treatments (Table S4), the latter including osmotic (salt) stress, changes in irradiance or relative humidity, and deficiencies or sufficiencies for various nutrients (nitrogen, phosphorus, K^+, sulfur, iron) or O_2. None of seven treatments found to decrease Lp_r altered the phenotypic difference between Col-0 and *hcr1* (Figure S3D). Among the other conditions tested, K^+ starvation led to an ~20% increase of Lp_r in Col-0, consequently phenocopying *hcr1* Lp_r phenotype, while the mutant remained insensitive to this treatment (Figure S3E). Treatment with cesium chloride, a blocker of K^+ channels (Broadley et al., 2001), recapitulated the differential K^+ starvation response of Col-0 and *hcr1* (Figure S3E). Col-0 and *hcr1* showed similar K^+ content in roots (Figure S3F) indicating that *hcr1* has a genuine defect in external K^+ perception, thereby lacking negative effects of K^+ on Lp_r observed in *Arabidopsis* (Col-0) and other plant species (Wang et al., 2013). We also found that bubbling air into the root bathing solution, similar to K^+ starvation, increased Lp_r in Col-0, to values similar to those in *hcr1*, while having no effects on the latter genotype (Figures 2C and S3E). Air bubbling was not used in standard conditions, to avoid root mechanical disturbance and thereby achieve homogeneous plant growth, a prerequisite for accurate Lp_r QTL mapping. However, positive effects of air bubbling on Lp_r suggested that our standard conditions were somewhat O_2 deficient. This was corroborated by a partial pressure for O_2, which was significantly lower than that in air bubbling conditions (standard: pO_2 = 11.1% ± 1.1%; bubbling: pO_2 = 20.1% ± 0.3%). By convention, the two growth conditions are now referred as hypoxia and normoxia, respectively. Interestingly, coupling of K^+ starvation with normoxia did

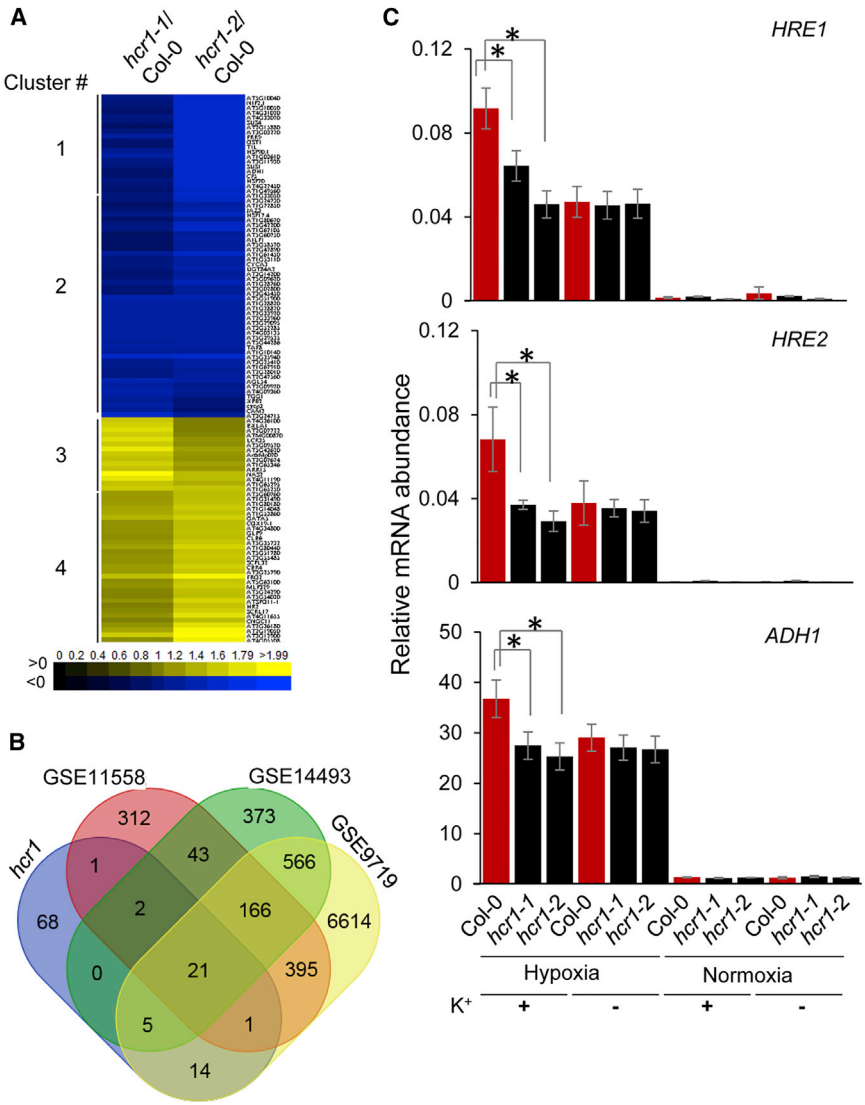

Figure 3. *HCR1* Mediates Potassium-Dependent Anaerobic Transcriptional Response

(A) Genes deregulated in *hcr1* with respect to Col-0. Plants were grown under K^+-replete hypoxia. Genes with transcript abundance showing >1.5-fold variation from Col-0 ($p < 0.05$; ANOVA) in at least one *hcr1* allelic mutant were considered as deregulated. The figure shows a hierarchical cluster analysis of 112 deregulated genes.

(B) De-regulated mRNAs in *hcr1* overlap with hypoxia-responsive mRNAs in Col-0 roots. Transcriptomic data for response of Col-0 roots to hypoxia were exported from Gene Expression Omnibus (GEO): GSE11558 (van Dongen et al., 2009), GSE14493 (Mustroph et al., 2009), and GSE9719 (Branco-Price et al., 2008). The Venn diagram shows the overlaps between these datasets and the deregulated mRNAs in *hcr1*.

(C) mRNA abundance of hypoxia marker genes in roots of Col-0 and *hcr1* plants exposed to various O_2 and K^+ availabilities (see legend of Figure 2C). Transcript levels of *HRE1*, *HRE2*, and *ADH1* were determined by qRT-PCR using gene specific primer pairs and are expressed relative to the average transcript abundance of *UBQ10* and F-box family protein (means ± SE, n = 6–12, N = 3). See also Figure S4.

not result in additive effect on Lp_r (Figure 2C). Thus, K^+ and O_2 act oppositely on Lp_r through common signaling pathways involving *HCR1*.

HCR1 Mediates a General K^+-Dependent Transcriptional Response to O_2 Deficiency

To gain further insights into the molecular function of *HCR1*, a comparative transcriptomic analysis was performed using Col-0 and *hcr1* plants grown under conditions where *HCR1* acts on Lp_r *i.e.* K^+-replete hypoxia. Genome-wide expression analysis based on gene chip hybridization uncovered deregulation of 112 genes in *hcr1* mutants as compared to Col-0 (>1.5-fold change at $p < 0.05$ in at least one *hcr1* allele) (Figure 3A; Table S5). These results were validated for a few selected genes using qRT-PCR (Figure S4). Gene ontology (GO) analysis revealed that genes deregulated in *hcr1* had significant enrichment in biological processes related to O_2 levels (Table S6). Hierarchical cluster analysis showed that all of the genes related to GO term "oxygen" belonged to cluster 1, the most strongly downregulated mRNAs in *hcr1* as compared to Col-0 (Figure 3A). This prompted us to compare the deregulated transcriptome of *hcr1* to three transcriptomic datasets in *Arabidopsis* roots under hypoxia (Branco-Price et al., 2008; van Dongen et al., 2009; Mustroph et al., 2009) (Figure 3B). Interestingly, 44 (39%) and 21 (19%) of the 112 genes that are deregulated in *hcr1* were responsive to hypoxia in at least one or all three studies, respectively. We next used qRT-PCR and investigated a core set of six typical hypoxia-responsive genes (HRGs) encoding TFs *HRE1* and *HRE2*, sucrose synthetases (*SUS1* and *SUS4*), and fermentative enzymes [*alcohol dehydrogenase 1* (*ADH1*), *pyruvate decarboxylase 1* (*PDC1*)] (Figures 3C and S4, upper panel). All showed a consistent downregulation in the two *hcr1* alleles. Thus, *hcr1* plants show a reduced molecular response to hypoxia indicating that *HCR1* positively regulates the core anaerobic transcriptional response. Since Lp_r of Col-0 is downregulated in response to O_2 deficiency (Figure 2C), the enhanced Lp_r of *hcr1* with respect to Col-0 can also be interpreted as a reduced sensitivity to this stress. Surprisingly, the gene chip analysis did not reveal any deregulation in *hcr1* of genes related to K^+ homeostasis. To further investigate root response to K^+, we used qRT-PCR and searched for a possible interplay between K^+ and O_2 availabilities during transcriptional response of typical HRGs. As shown in Figure 3C, *HRE1*, *HRE2*, and *ADH1* were strongly induced by hypoxia, and 30%–60% of this induction was dependent

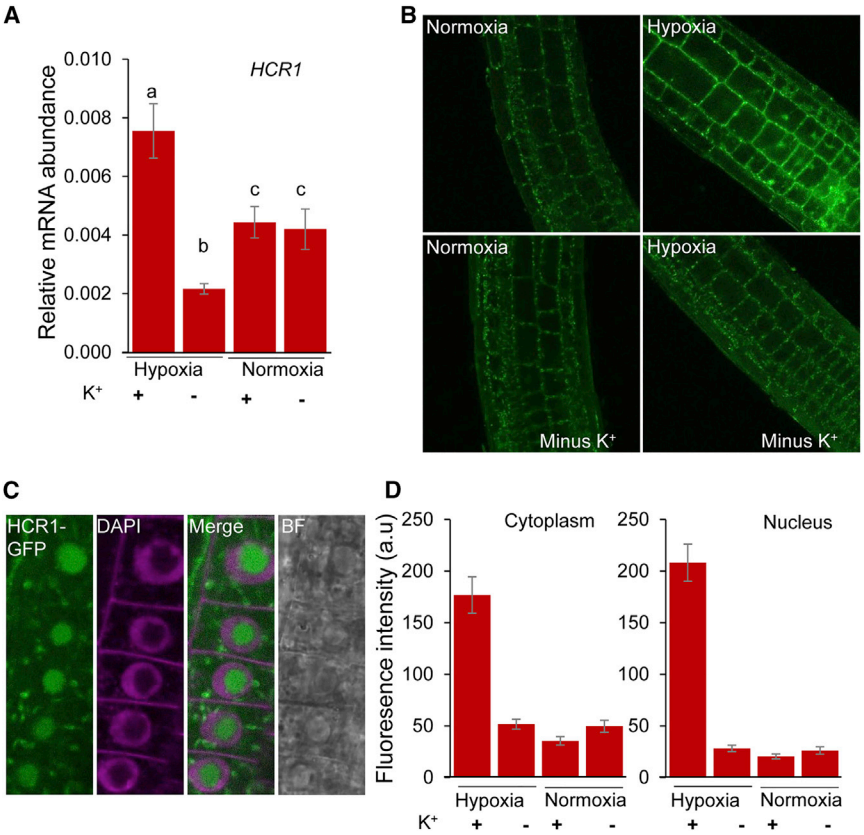

Figure 4. *HCR1* Is Regulated by Hypoxia in a K^+-Dependent Manner

(A) *HCR1* mRNA abundance in roots of Col-0 plants exposed to various conditions (see legend of Figure 2C). Mean *HCR1* transcript abundance (±SE) was quantified using qRT-PCR and expressed relative to the average transcript abundance of *UBQ10* and F-box family protein (n = 6, N = 3).

(B and C) Subcellular localization of a GFP-HCR1 fusion expressed in *hcr1* from a prom*HCR1*::GFP::HCR1 construct. Eight to 10-day-old seedlings were transferred to a medium with or without K^+ and further grown for 2 days. Hypoxia was generated by flushing N_2 into the petri dish for 2–3 hr. Three to four roots of several transgenic lines were observed in each indicated condition, and in three independent experiments. A representative image for each condition is shown (B). A higher magnification with DAPI staining was used to confirm the nucleolar localization of GFP-HCR1 (C).

(D) Fluorescence intensity in cytoplasm and nucleus of *hcr1* plants expressing a prom*HCR1*::GFP::HCR1 construct and grown under indicated conditions. The graph shows average signal intensities (±SE) in ≥110 cells from nine or more roots and three independent experiments.

upon the presence of K^+ in the medium. With respect to Col-0, the latter component was lacking in *hcr1* as the two genotypes showed similar transcriptional response under combined O_2 and K^+ deficiencies. Thus, *hcr1* shows a transcriptional phenotype exclusively under K^+-replete and O_2-deficient conditions, thereby offering a striking parallel to its Lp_r phenotype. These results uncover a link between K^+ and O_2 sensing in plants, which is fully dependent on *HCR1*.

HCR1 Expression Is Regulated by K^+ and O_2 Availabilities

Based on dependence on K^+ and low O_2 of *HCR1* roles in regulation of HRG expression and Lp_r, we hypothesized that both K^+ and O_2 could act as upstream signals regulating *HCR1*. The influence of O_2 and K^+ availability on *HCR1* mRNA regulation was investigated using qRT-PCR. K^+ availability increased by 3.6-fold the abundance of *HCR1* mRNA under hypoxia but was without effects under normoxia (Figure 4A). O_2 deficiency enhanced *HCR1* mRNA levels by 1.7-fold under K^+-sufficient conditions but had opposite effects under K^+-deficient conditions (Figure 4A). These data highlight a tight interplay between O_2 and K^+ in regulating *HCR1* expression. Expression at protein level was probed using a GFP-tagged HCR1 (from Col-0) expressed under the native *HCR1* promoter (*promHCR1*::GFP::HCR1). Visualization in roots using confocal laser scanning microscopy revealed a dual sub-cellular localization of GFP-HCR1, in the cytoplasm and nucleus (Figure 4B). A particularly high accumulation of GFP-HCR1 was observed in the nucleolus as revealed by complementary DAPI staining (Figure 4C). Quantitative measurements indicated that the GFP-HCR1 fluorescence signal was enhanced by hypoxia in both cytoplasm (5-fold) and nucleus (10-fold), but only in the presence of K^+ (Figure 4D). Thus, combined O_2 deficiency and K^+ sufficiency seem to lead to maximal *HCR1* mRNA and protein accumulations. This expression profile matches the role of *HCR1* in orchestrating anaerobic transcriptional response and root hydraulics, specifically under K^+-replete hypoxic conditions.

HCR1 Is a Molecular Switch to Adjust Plant Water Relations under Various Flooding Conditions

The question why plants adjust Lp_r when exposed to hypoxia remains disputed (Holbrook and Zwieniecki, 2003; Shabala et al., 2014). In nature, hypoxia can be induced by soil flooding (waterlogging) or plant submergence, two contexts having contrasting effects on plant transpiration and thereby on root water uptake. K^+ plays a key role in cell turgor and elongation (expansive growth), which both require optimized tissue hydraulics. Thus, the dependence of Lp_r on hypoxia and K^+-availability may underlie tight links between water relations, hypoxia, and plant growth. To address these links and a possible role of *HCR1*, we developed an in vitro assay using a stagnant solution (pO_2 = 10.5% ± 0.7%) (Wiengweera and Greenway, 2004) to induce hypoxia, selectively to root systems (waterlogging) or to whole plants (submergence). The effects of K^+ availability were investigated in these two contexts. With respect to plants with aerated roots, waterlogging induced a dramatic reduction in shoot fresh

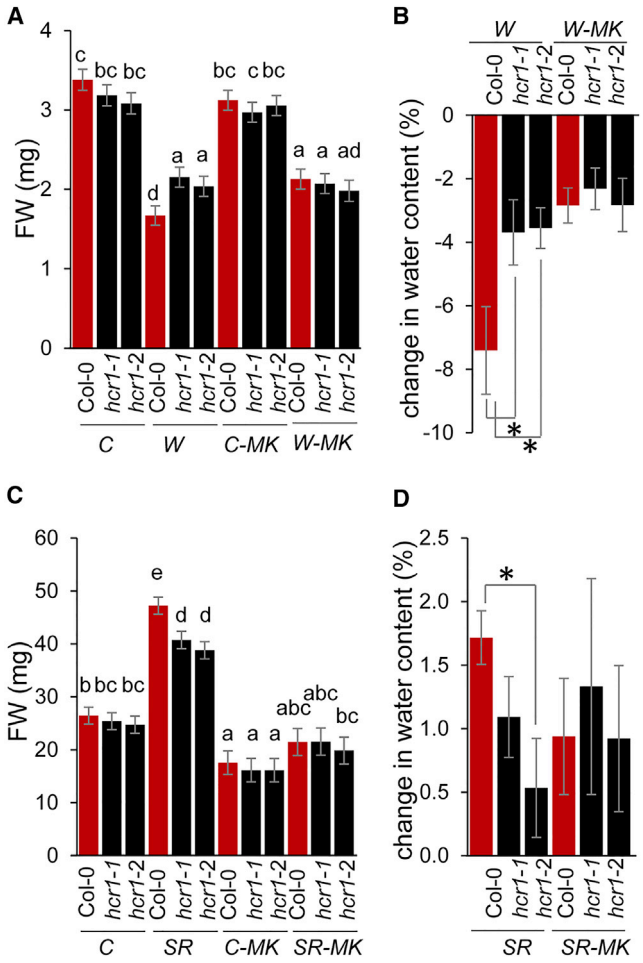

Figure 5. *HCR1* Differentially Controls Shoot Water Relations and Growth under Distinct Hypoxia Scenarios

(A and B) Shoot water relations during waterlogging. Ten-day-old Col-0 and *hcr1* plants were grown for 3 hr in vitro, either vertically at the surface of a 0.7% agar solution (control: *C*) or by embedding roots in a 0.1% agar stagnant solution (waterlogging: *W*). In either case, shoots were exposed to a flow of dry air (RH = 23% ± 3%) and their fresh weight (±SE) was measured (A). For minus K^+ (*MK*) condition, 8-day-old plants were transferred to a medium lacking K^+ for 2 days prior to measurement of shoot fresh weight as indicated above. Changes in water content induced by waterlogging were calculated (in %; ± SE) for each genotype by reference to the corresponding control conditions (B). Data from n = 16–19, N = 2. Dry weight data are shown in Figure S5D.

(C and D) Shoot water relations during recovery from submergence. Ten-day-old Col-0 and *hcr1* plants were grown for 4 days in control (*C*) or fully submerged (*SR*) conditions in the presence or absence (*MK*) of K^+. Plants were then transferred to aerated conditions (0.7% agar medium) and shoot fresh weight (C) and change in water content (D) were determined after 4 days. Same conventions as in (A) and (B). Data from n = 9–23, N = 2. See also Figures S5A–S5C and S5E for submergence studies.

See also Figure S5.

weight (Figure 5A) and water content (Figure 5B). In Col-0, this reduction was higher under K^+-replete than K^+-deficient conditions. We also noticed that this reduction was more pronounced in Col-0 than *hcr1,* specifically under K^+-replete conditions. Thus, *hcr1* shows a better shoot water status than Col-0 under O_2-deficient K^+-replete conditions. This performance is consistent with a higher Lp_r in the mutant genotype, specifically in these conditions. Next, we compared the tolerance of Col-0 and *hcr1* to submergence by checking their recovery under aerated conditions. Strikingly, this treatment stimulated growth of the two genotypes with a 2-fold increase in fresh weight in the presence of K^+ (Figure 5C). Col-0 exhibited a better shoot growth and water content than *hcr1* in these conditions, whereas the two genotypes showed a similar reduced growth on a K^+-deficient medium (Figures 5C and 5D). The capacity to recover from submergence, better in Col-0 than *hcr1*, matches their differences in anaerobic transcriptional response, specifically under K^+-replete conditions. A growth advantage of Col-0 over *hcr1* was also observed during recovery of soil grown plants from submergence, conditions supposed to be non-limiting for K^+ (Figures S5A–S5C). It is of note that Col-0 and *hcr1* did not differ significantly for shoot dry weight during both in vitro and soil experiments (Figures S5B, S5D, and S5E), suggesting a specific role of *HCR1* in expansive growth, consistent with its involvement in regulation of hydraulics. Moreover, the differential growth of the two genotypes matches their K^+-dependent difference in root hydraulics and transcriptional responses to hypoxia. Overall, these studies highlight strong links between O_2 and K^+ availability on the one hand and plant growth and water content on the other hand. Phenotypic differences between Col-0 and *hcr1* indicate how *HCR1* contributes to adjusting the plant's hypoxia response to its growth potential as determined by K^+ availability and the type of water demand. The differential performance of Col-0 and *hcr1*, under waterlogging or submergence scenarios, illustrates the distinct adaptive values of both active and inactive alleles of *HCR1*.

HCR1 Affects Lp_r through RAP2.12

HRE1 and *HRE2* are ERF-VII TFs mediating hypoxia signaling. Their dramatic transcriptional deregulation in *hcr1* (Figure 3C) suggested that *HCR1* is likely involved in one of most early events of plant anaerobic transcriptional response. *RAP2.12* along with its close homologs *RAP2.2* and *RAP2.3* have been identified as key upstream regulators of this response (Bui et al., 2015; Gasch et al., 2016). In contrast to *HRE*s, mRNA abundance of ERF-VII *RAP2s* was neither dependent on O_2 availability nor on *HCR1* function (Figures 6A and S6A). However, western blot analyses of plants grown under K^+-replete hypoxia revealed a 2-fold lesser abundance of RAP2.12 protein in *hcr1* mutants as compared to Col-0 (Figures 6B and 6C). We therefore hypothesized that *RAP2.12* could be a target for *HCR1*-mediated hypoxia signaling, thereby stabilizing the protein. In line with this, the purified kinase domain of HCR1 was able to phosphorylate the full-length RAP2.12 protein and a peptide (pep27) covering part of its N-terminal region (Figures 6D and 6E). Modified forms of pep27 where the Ser or Thr residues were individually mutated to Ala identified Thr20 as a putative phosphorylation site for HCR1 (Figure 6E). At the whole-root level, downregulated anaerobic transcriptional response and higher Lp_r in *hcr1* could be the outcome of lesser abundance of RAP2.12. To test this hypothesis, we investigated a RAP2.12-overexpressing transgenic line (Licausi et al., 2011). This

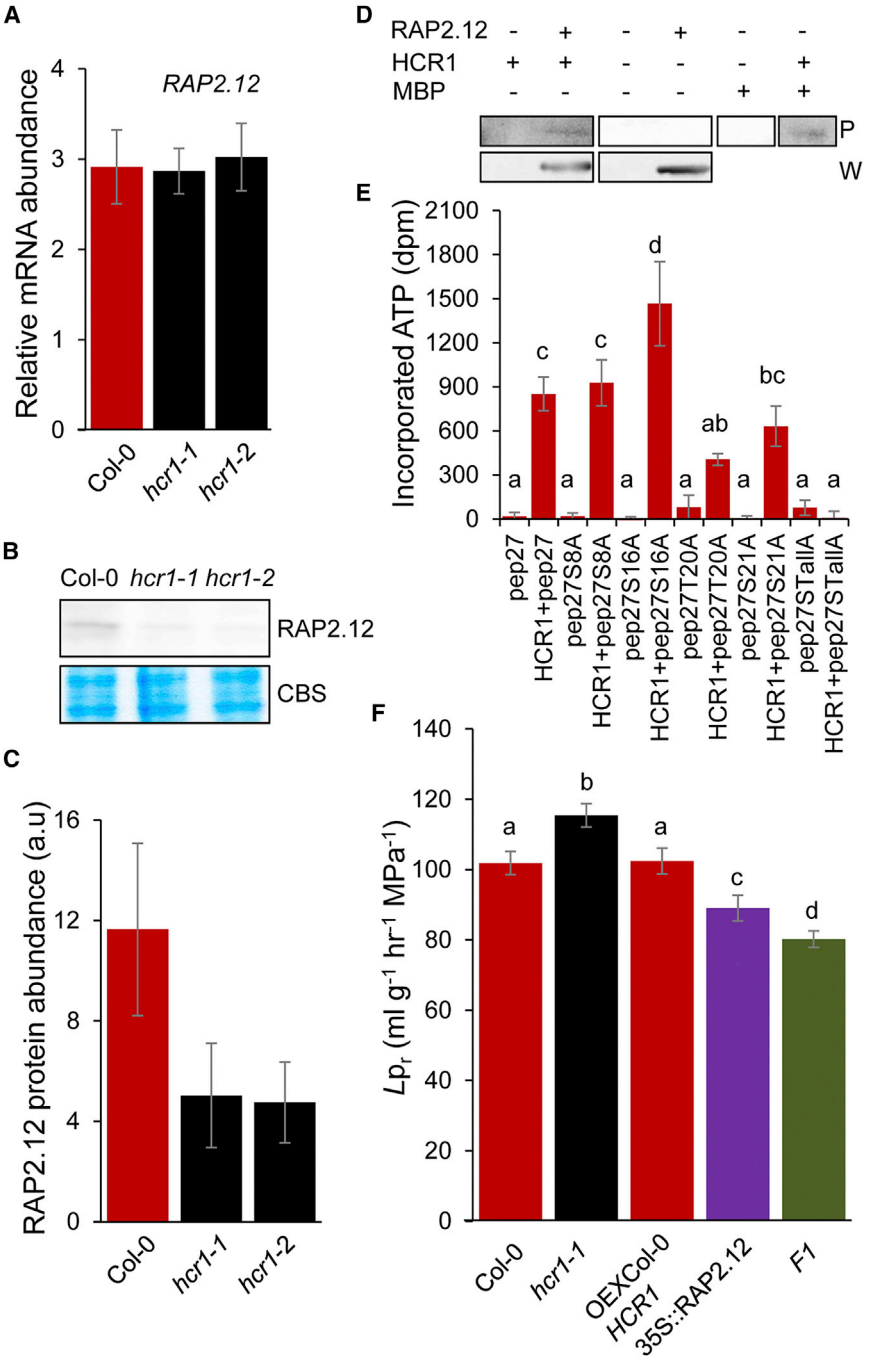

Figure 6. *HCR1* Regulates RAP2.12

(A) *RAP2.12* mRNA abundance in the roots of Col-0 and *hcr1* plants grown under K^+-replete hypoxia. Mean transcript levels (±SE) are expressed relative to the average transcript levels of *UBQ10* and F-box family protein (n = 6, N = 3) (see also Figure S6A).

(B and C) Western blot analysis of RAP2.12 expression (along with corresponding Coomassie-blue-stained gel [CBS]) (B) in roots from Col-0 and *hcr1* plants grown under K^+-replete hypoxia conditions and corresponding protein quantification (means ± SE, n = 5, N = 5) (C).

(D and E) In vitro phosphorylation of RAP2.12 by recombinant kinase domain of HCR1 ($HCR1_{821–1117}$). In (D), upper panel shows phosphorylation (P) by recombinant HCR1 kinase domain of full-length RAP2.12 protein blotted onto a membrane. MBP was used as a positive control in these experiments. Membrane was cut around the size of proteins of interest (RAP2.12 and MBP). Membrane pieces were then treated in parallel for phosphorylation assay and subsequent imaging. Lower panel shows western blot detection (W) of RAP2.12 protein on corresponding membrane pieces using anti-RAP2.12 antibodies. In (E), N-terminal RAP2.12 peptides either native (pep27) or carrying the indicated mutations were tested for phosphorylation by HCR1. pep27STallA corresponds to a quadruple Ala mutant at positions 8, 16, 20, and 21. Means (±SE) of incorporated ATP in these peptides are shown (n = 6, N = 3).

(F) Lp_r in plants overexpressing *HCR1* (OEXCol-0 HCR1) or RAP2.12 (35S::RAP2.12) or in the F1 progeny of a cross between these overexpressors. All measurements were performed under K^+-replete hypoxia (means ± SE, n ≥ 18, N = 3) (see also Figures S6B–S6D).

See also Figure S6.

genotype showed a lower Lp_r (Figures 6F and S6B) and higher induction of HRGs (Figure S6C) than Col-0 under K^+-replete hypoxic conditions whereas no Lp_r phenotype was observed under K^+-depleted or normoxia conditions (Figure S6B). Overall, mRNA abundance of four typical HRGs (*ADH*, *PDC1*, *HRE1*, *HRE2*) was correlated with Lp_r in Col-0, *hcr1*, and 35S::RAP2.12 plants under K^+-replete hypoxia (Figure S6C). Thus, *RAP2.12*- and *HCR1*-mediated inhibition of Lp_r show similar dependencies on O_2 and K^+ availabilities, supporting the idea that *RAP2.12* and *HCR1* contribute to the same signaling pathway. Intriguingly, transgenic lines overexpressing Col-0 *HCR1* under the control of an endogenous or d35S promoter did not exhibit lower Lp_r than Col-0 plants under K^+-replete hypoxia (Figures 6F, S2C, and S6D). In addition, d35S::HCR1 plants showed similar *L*pr as *hcr1-1* plants under K^+-depleted or normoxic conditions. The overall data suggest that, in Col-0, the accumulation profile of *HCR1* mRNA is not limiting for mediating root responses to hypoxia. To search for additional functional links between *HCR1* and *RAP2.12*, we performed reciprocal crosses of one of the *HCR1*-overexpressing lines with the RAP2.12-overexpressing line. Interestingly, F1 plants originating from these crosses showed a stronger inhibition of Lp_r than the parental lines (Figure 6F). These studies provide strong genetic evidence that *HCR1* and *RAP2.12* can be co-limiting in Lp_r inhibition under K^+-replete hypoxia. Further, it is recognized that *HCR1* integrates K^+ and O_2 signaling to regulate *RAP2.12*-mediated hydraulic response of roots to hypoxia.

DISCUSSION

Quantitative Genetics of Plant Hydraulics Unravels Molecular Bases of Combinatorial Root Signaling

In the present study, we used a quantitative genetics approach to search for genetic elements controlling plant root hydraulics. This approach proved to be highly challenging: the natural variation of plant biophysical traits such as Lp_r had never been explored to this extent, primarily due to the difficulty of phenotyping these traits at high throughput. In addition, their genetic tractability can be dominated by a strong dependence on the environment (Sutka et al., 2011). To address these issues, we have used highly standardized procedures for plant growth in hydroponic conditions and have optimized the throughput of Lp_r measurements, with several pressure chambers running in parallel. These procedures allowed us to map three QTLs for Lp_r in an *Arabidopsis* RIL population. The identification of QTLs for Lp_r is considered to be a significant advance in the field. Much broader genomic regions controlling root hydraulics were previously reported in rice using chromosome segment substitution lines (Adachi et al., 2010).

Fine mapping of a Lp_r QTL (Lprm320), which acts through modulation of plant root aquaporin activity, led to a genomic region containing five genes, including *HCR1*. Quantitative and molecular complementation tests validated *HCR1* as the quantitative trait gene corresponding to Lprm320. In particular, phenotypic expression in a Col-0 *hcr1* knockout mutant showed that the Bur-0 *HCR1* allele is hyperfunctional with respect to its Col-0 counterpart. An extended search for *HCR1* natural variation revealed the existence at the species-wide level of at least seven *HCR1* alleles, of which two (H3: Fei-0; H4: Zu-1) seem to be functionally inactive in a Col-0 background. An inactivating mutation at residue 1072 was potentially identified in the Fei-0 form. These natural variations indicate that we have identified a gene with allelic forms determine up to 20% of *Arabidopsis* root hydraulics, with significance at the species level. Interestingly, the presence of an allelic series in *HCR1* is a feature shared with several plant genes of well-established adaptive significance (Alonso-Blanco and Méndez-Vigo, 2014).

Plant Raf-like MAPKKK form a large multigenic family with 64 members in *Arabidopsis*, divided in two main classes (B, C) and 11 subgroups (Ichimaru and MAPK group, 2002). *HCR1* belongs to subgroup B4. It is distantly related to *Constitutive Triple Response 1* (*CTR1*), a B3 subgroup member, involved in ethylene signaling (Ichimaru and MAPK group, 2002). The few other plant Raf-like MAPKKK characterized so far play various roles in plant defense, abiotic stress, or hormone signaling (Sinha et al., 2011; Rodriguez et al., 2010). In their natural habitats, plants continuously face multiple environmental constraints and need to integrate inputs from different sensing and signaling pathways. Involvement of Raf-like MAPKKK in these processes is emerging. For instance, *CTR1* is shown to regulate cross-talks between multiple hormonal signals including ethylene, abscisic acid, gibberellic acid, and auxin (Zhong and Chang, 2012). Although of upmost importance for higher plant growth and survival, signaling mechanisms underlying integration of soil born signals remain largely unknown. Lp_r, which is controlled by multiple edaphic signals, proved to be a relevant trait to address these questions. The identification of *HCR1* as a Raf-like MAPKKK suggested that we had cloned a key signaling gene acting as a master regulator of aquaporins. A large-scale phenotypic screen confirmed this and uncovered roles of *HCR1* in response of Lp_r to both K^+ and O_2 availability. Although K^+ and O_2 initially appeared as unrelated signals for plant water transport regulation, our study revealed a role of *HCR1* in root hydraulic responses, specifically under K^+-replete O_2-deficient conditions. Thus, *HCR1* mediates a cross-talk of abiotic signaling in roots.

Insights into Low O_2 Sensing in Plants

Comparative transcriptomic analyses of Col-0 and *hcr1* plants indicated that, beyond its effects on Lp_r, *HCR1* acts on a fundamental cellular response to hypoxia and positively regulates the anaerobic transcriptional response. One of most striking results was that *HCR1*-mediated induction of HRGs paralleled *HCR1* effects on Lp_r and was strictly dependent upon K^+ availability. Thus, the overall work points to a pivotal role of *HCR1*, in integrating O_2 sensing with the availability of cations such as K^+ (Figure 7). We then took RAP2.12 as a representative isoform of ERF-VII RAP2s, which have partially redundant functions in activation of HRGs (Gasch et al., 2016). We further showed that, under K^+-replete O_2-deficient conditions, *HCR1* positively regulates the protein abundance of RAP2.12, without interfering with its mRNA abundance. *HCR1* is itself regulated by the interaction between O_2 and K^+ availabilities, at both mRNA and protein levels. Induction of HCR1 protein accumulation in nuclei, in particular, under K^+-replete O_2-deficient conditions, is coherent with the stabilization and nuclear relocalization of RAP2.12 observed in this context. We propose this effect of *HCR1* on abundance of RAP2.12 and possibly other RAP2s to be at least partially independent of the canonical N-end rule pathway of targeted proteolysis (Figure 7) (Gibbs et al., 2011; Licausi et al., 2011). Indeed, deregulated transcriptome of *hcr1* shares 2-fold higher similarity with that of knock-down lines for *RAP2.2-12* than genotypes altered in components of the N-end rule pathway such as *proteolysis 6* (*prt6*) or plants overexpressing *Plant Cysteine Oxidase 1* (35S::PCO1) (Figure S7A). Under normoxia, RAP2.12 is sequestered at the plasma membrane by association with Acyl-CoA Binding Proteins 1 and 2, whereas, under hypoxia, it may interact with other partners for nuclear translocation (Gibbs et al., 2015). Here, we speculate that HCR1 may phosphorylate RAP2.12 itself or one of protein partners involved in its stabilization. In line with the former hypothesis, RAP2.12 can be recognized by the HCR1 kinase domain in vitro. ERF6 and ERF104, two distant homologs of RAP2.12 in *Arabidopsis*, and SUB1A1, an ERF-VII in rice, are phosphorylated through a MPK3/MPK6 signaling cascade, resulting in their enhanced stability or activity (Bethke et al., 2009; Meng et al., 2013; Singh and Sinha, 2016).

The mode of action of HCR1 on Lp_r and aquaporins may well be more indirect. We previously showed that hypoxia results in a sudden inhibition of Lp_r through cytosolic acidification and H^+-dependent gating of aquaporins (Tournaire-Roux et al., 2003). However, plant roots are able to re-adjust cytosolic pH under prolonged low-O_2 conditions (Greenway and Gibbs, 2003). In our experiments, plant roots were exposed to hypoxia

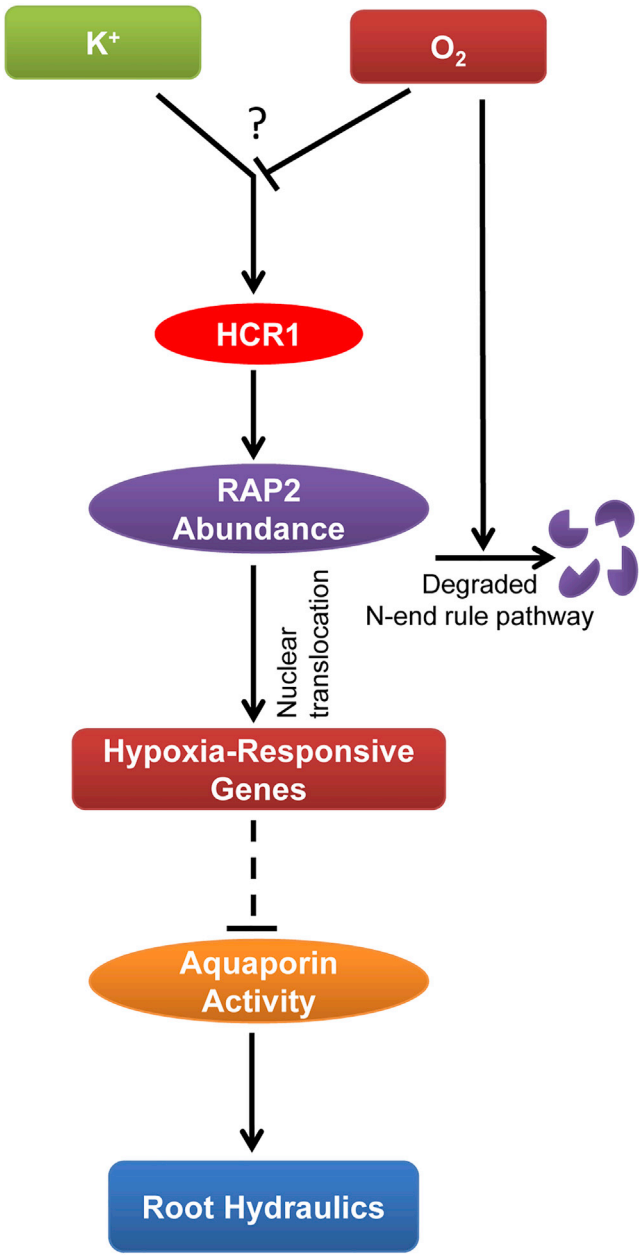

Figure 7. A Schematic Model for the Role of *HCR1* in Regulation of Root Hydraulics

Primary activation of HRGs (hypoxia-responsive genes) under limiting O_2 is achieved by stabilization and nuclear translocation of RAP2s (Bui et al., 2015; Gasch et al., 2016; Licausi et al., 2011), which are degraded via a N-end rule pathway in the presence of sufficient O_2 concentration. Accumulation of HCR1 is induced by hypoxia only in K^+-replete conditions and positively regulates RAP2 abundance. It thereby contributes to the induction of HRGs. The upstream molecular mechanisms that link K^+ and O_2 availability to HCR1 regulation remain to be identified. The resulting K^+-dependent anaerobic transcriptional response per se negatively regulates aquaporin activity through unknown mechanisms that cause a downregulation of Lp_r.
See also Figure S7.

for about 2 weeks, and cytosolic pH of *hcr1* was found to be similar to that of Col-0 (Figures S7B and S7C). Since *HCR1*-mediated downregulation of Lp_r was not due to cytosolic acidification, we hypothesized that it might be linked to the lower abundance of RAP2.12 and possibly other ERF-VII RAP2s (Figure 7). Consistently, overexpression of RAP2.12 in Col-0 resulted in an enhanced downregulation of Lp_r under hypoxia, which was even more pronounced in lines co-overexpressing *HCR1* and RAP2.12. Thus, we provide genetic evidence for a mechanism for long-term regulation of Lp_r under K^+-replete hypoxic conditions, which involves induction of HRGs over a certain threshold but does not directly target aquaporin transcription (Table S5). In practical terms, genetic co-manipulation of *HCR1* and RAP2.12 allowed variation of plant root hydraulics by up to 30%.

Significance of Cation Availability in Plant Responses to Hypoxia

Because of its impact on cell energy and redox status, O_2 availability exerts well-known effects on transport and storage of ions such as K^+ (Shabala et al., 2014). Perturbations in K^+ homeostasis can thus contribute to metabolic alterations observed under hypoxia. However, the converse link between ion availability and O_2 sensing had never been explored in plants. In animals, transition metals and other cations (including K^+) can regulate HIF-1α, a key regulator of anaerobic transcriptional response, at both mRNA and protein levels, and this process seems to be mostly related to growth adaptation of cancer cells to hypoxic environments (Giaccia et al., 2003; Lan et al., 2007). The present study provides hints at the physiological impact and adaptive value of integrating hypoxia and K^+ signaling in plants. It is proposed that K^+-dependent effects of *HCR1* on tissue hydraulics imparts two sorts of adaptive strategies for plant growth and survival under hypoxia. The first strategy operates under hypoxia associated with a strong transpirational demand, such as waterlogging, during which having roots with high water permeability, like *hcr1*, prevents shoot dehydration. The other survival strategy, as shown by Col-0, is to have lesser water permeable roots and higher metabolic response to enhance plant tolerance to long-term submergence and favor subsequent growth recovery, in conditions with no or limited transpirational demand. In both cases, K^+ availability may serve as a signal that the soil is not washed out and favorable to subsequent plant growth. Although Bur-0 and Col-0 showed similar tolerance to submergence in an earlier studies (Vashisht et al., 2011), these and other *Arabidopsis* accessions have revealed various natural alleles of *HCR1*, with different functionalities with regard to regulating Lp_r. While genetic variation of ERF-VII TFs has proved central for improvement of rice performance in paddy fields (Gibbs et al., 2015), the present genetic and molecular studies lead us to propose that the HCR1-RAP2 molecular pathway could represent a relevant target for improving the resilience of other crops to flooding.

Open Questions

Our work reveals combinatorial signaling of O_2 and K^+ in plants and opens numerous questions.

- Though HCR1 accumulation profile parallels its signaling function, the molecular mechanisms that possibly allow

O_2 and K^+ signals to activate HCR1 protein kinase activity remain to be investigated.

- Whereas RAP2.12 can be phosphorylated by HCR1 in vitro, the existence and the significance of RAP2 phosphorylation during O_2 sensing in plants is not yet determined.
- Exploring the function of HCR1 natural variants in vitro and in vivo may advance our understanding about the mode of action of HCR1. Extensive studies on a broad set of accessions will be needed to establish the distinct adaptive values of these variants under variable flooded conditions.

STAR★METHODS

Detailed methods are provided in the online version of this paper and include the following:

- KEY RESOURCES TABLE
- CONTACT FOR REAGENT AND RESOURCE SHARING
- EXPERIMENTAL MODEL AND SUBJECT DETAILS
- METHOD DETAILS
  - Growth Conditions
  - Plant Phenotyping for Water Relations
  - QTL and Fine Mapping
  - Quantitative and Molecular Complementation
  - Microarray Analysis
  - Quantitative Real Time-PCR
  - GUS Assays
  - Western Hybridization
  - Sub-cellular Localization of HCR1
  - pH Measurements
  - Protein Purification and Kinase Assays
  - Determination of Cation Accumulation
- QUANTIFICATION AND STATISTICAL ANALYSIS
- DATA AND SOFTWARE AVAILABILITY
  - Data Resource

SUPPLEMENTAL INFORMATION

Supplemental Information includes seven figures and seven tables and can be found with this article online at http://dx.doi.org/10.1016/j.cell.2016.08.068.

AUTHOR CONTRIBUTIONS

The experiments were conceived and designed by Z.S., O.L., and C.M. and mainly carried out by Z.S. Genetic materials for fine mapping were generated by M.C.. C.T.-R. performed protein production and kinase assays. C.T.-R. and M.C. contributed equally to the work. A.M. and Y.B. contributed to confocal microscopy and QTL mapping, respectively. Z.S., C.T.-R., A.M., O.L., and C.M. analyzed the data. Z.S. and C.M. wrote the paper.

ACKNOWLEDGMENTS

This work was supported by the Agence Nationale de la Recherche (ANR-11-BSV6-018) and a research contract from Syngenta (HydroRoot). The IJPB benefits from the support of the Labex Saclay Plant Sciences-SPS (ANR-10-LABX-0040-SPS). We thank Dr. Francesco Licausi for providing plant materials and critical reading of the manuscript, Dr. Elodie Marchadier for advice on QTL analysis, and Dr. Sandrine Ruffel for help on microarray analysis. The technical assistance of Céline Rançon and Xavier Dumond for plant growth and transformations is fully acknowledged.

Received: March 18, 2016
Revised: August 1, 2016
Accepted: August 25, 2016
Published: September 15, 2016

REFERENCES

Adachi, S., Tsuru, Y., Kondo, M., Yamamoto, T., Arai-Sanoh, Y., Ando, T., Ookawa, T., Yano, M., and Hirasawa, T. (2010). Characterization of a rice variety with high hydraulic conductance and identification of the chromosome region responsible using chromosome segment substitution lines. Ann. Bot. (Lond.) *106*, 803–811.

Alonso-Blanco, C., and Méndez-Vigo, B. (2014). Genetic architecture of naturally occurring quantitative traits in plants: an updated synthesis. Curr. Opin. Plant Biol. *18*, 37–43.

Arends, D., Prins, P., Broman, K.W., and Jansen, R.C. (2014). Tutorial - Multiple-QTL Mapping (MQM) analysis for R / qtl. http://www.rqtl.org/tutorials/MQM-tour.pdf. 1–39.

Aroca, R., Porcel, R., and Ruiz-Lozano, J.M. (2012). Regulation of root water uptake under abiotic stress conditions. J. Exp. Bot. *63*, 43–57.

Bethke, G., Unthan, T., Uhrig, J.F., Pöschl, Y., Gust, A.A., Scheel, D., and Lee, J. (2009). Flg22 regulates the release of an ethylene response factor substrate from MAP kinase 6 in *Arabidopsis thaliana* via ethylene signaling. Proc. Natl. Acad. Sci. USA *106*, 8067–8072.

Branco-Price, C., Kaiser, K.A., Jang, C.J.H., Larive, C.K., and Bailey-Serres, J. (2008). Selective mRNA translation coordinates energetic and metabolic adjustments to cellular oxygen deprivation and reoxygenation in *Arabidopsis thaliana*. Plant J. *56*, 743–755.

Broadley, M.R., Escobar-Gutiérrez, A.J., Bowen, H.C., Willey, N.J., and White, P.J. (2001). Influx and accumulation of Cs^+ by the *akt1* mutant of *Arabidopsis thaliana* (L.) Heynh. lacking a dominant K^+ transport system. J. Exp. Bot. *52*, 839–844.

Bui, L.T., Giuntoli, B., Kosmacz, M., Parlanti, S., and Licausi, F. (2015). Constitutively expressed ERF-VII transcription factors redundantly activate the core anaerobic response in *Arabidopsis thaliana*. Plant Sci. *236*, 37–43.

Gasch, P., Fundinger, M., Müller, J.T., Lee, T., Bailey-Serres, J., and Mustroph, A. (2016). Redundant ERF-VII transcription factors bind an evolutionarily-conserved cis-motif to regulate hypoxia-responsive gene expression in Arabidopsis. Plant Cell *28*, 160–180.

Giaccia, A., Siim, B.G., and Johnson, R.S. (2003). HIF-1 as a target for drug development. Nat. Rev. Drug Discov. *2*, 803–811.

Gibbs, D.J., Lee, S.C., Isa, N.M., Gramuglia, S., Fukao, T., Bassel, G.W., Correia, C.S., Corbineau, F., Theodoulou, F.L., Bailey-Serres, J., and Holdsworth, M.J. (2011). Homeostatic response to hypoxia is regulated by the N-end rule pathway in plants. Nature *479*, 415–418.

Gibbs, D.J., Conde, J.V., Berckhan, S., Prasad, G., Mendiondo, G.M., and Holdsworth, M.J. (2015). Group VII Ethylene Response Factors co-ordinate oxygen and nitric oxide signal transduction and stress responses in plants. Plant Physiol. *169*, 23–31.

Greenway, H., and Gibbs, J. (2003). Mechanisms of anoxia tolerance in plants. II. Energy requirements for maintenance and energy distribution to essential processes. Funct. Plant Biol. *30*, 999–1036.

Holbrook, N.M., and Zwieniecki, M.A. (2003). Plant biology: Water gate. Nature *425*, 361.

Ichimaru, K., and MAPK group. (2002). Protein kinase cascades in plants: MAPK Group. Trends Plant Sci. *7*, 301–308.

Koffler, B.E., Luschin-Ebengreuth, N., Stabentheiner, E., Müller, M., and Zechmann, B. (2014). Compartment specific response of antioxidants to drought stress in Arabidopsis. Plant Sci. *227*, 133–144.

Lan, M., Shi, Y., Sun, L., Liu, L., Guo, X., Lu, Y., Wang, J., Liang, J., and Fan, D. (2007). KCl depolarization increases HIF-1 transcriptional activity via the calcium-independent pathway in SGC7901 gastric cancer cells. Tumour Biol. *28*, 173–180.

Licausi, F., van Dongen, J.T., Giuntoli, B., Novi, G., Santaniello, A., Geigenberger, P., and Perata, P. (2010). HRE1 and HRE2, two hypoxia-inducible ethylene response factors, affect anaerobic responses in *Arabidopsis thaliana*. Plant J. *62*, 302–315.

Licausi, F., Kosmacz, M., Weits, D.A., Giuntoli, B., Giorgi, F.M., Voesenek, L.A., Perata, P., and van Dongen, J.T. (2011). Oxygen sensing in plants is mediated by an N-end rule pathway for protein destabilization. Nature *479*, 419–422.

Maurel, C., Boursiac, Y., Luu, D.-T., Santoni, V., Shahzad, Z., and Verdoucq, L. (2015). Aquaporins in plants. Physiol. Rev. *95*, 1321–1358.

Meng, X., Xu, J., He, Y., Yang, K.-Y., Mordorski, B., Liu, Y., and Zhang, S. (2013). Phosphorylation of an ERF transcription factor by Arabidopsis MPK3/MPK6 regulates plant defense gene induction and fungal resistance. Plant Cell *25*, 1126–1142.

Mustroph, A., Zanetti, M.E., Jang, C.J.H., Holtan, H.E., Repetti, P.P., Galbraith, D.W., Girke, T., and Bailey-Serres, J. (2009). Profiling translatomes of discrete cell populations resolves altered cellular priorities during hypoxia in Arabidopsis. Proc. Natl. Acad. Sci. USA *106*, 18843–18848.

Nakano, T., Suzuki, K., Fujimura, T., and Shinshi, H. (2006). Genome-wide analysis of the ERF gene family in Arabidopsis and rice. Plant Physiol. *140*, 411–432.

Rodriguez, M.C., Petersen, M., and Mundy, J. (2010). Mitogen-activated protein kinase signaling in plants. Annu. Rev. Plant Biol. *61*, 621–649.

Shabala, S., Shabala, L., Barcelo, J., and Poschenrieder, C. (2014). Membrane transporters mediating root signalling and adaptive responses to oxygen deprivation and soil flooding. Plant Cell Environ. *37*, 2216–2233.

Singh, P., and Sinha, A.K. (2016). A positive feedback loop governed by SUB1A1 interaction with MITOGEN ACTIVATED PROTEIN KINASE 3 imparts submergence tolerance in rice. Plant Cell *28*, 1127–1143.

Sinha, A.K., Jaggi, M., Raghuram, B., and Tuteja, N. (2011). Mitogen-activated protein kinase signaling in plants under abiotic stress. Plant Signal. Behav. *6*, 196–203.

Sutka, M., Li, G., Boudet, J., Boursiac, Y., Doumas, P., and Maurel, C. (2011). Natural variation of root hydraulics in Arabidopsis grown in normal and salt-stressed conditions. Plant Physiol. *155*, 1264–1276.

Tadege, M., Dupuis, I., and Kuhlemeier, C. (1999). Ethanolic fermentation: New functions for an old pathway. Trends Plant Sci. *4*, 320–325.

The 1001 Genomes Consortium (2016). 1,135 genomes reveal the global pattern of polymorphism in *Arabidopsis thaliana*. Cell *166*, 481–491.

Tournaire-Roux, C., Sutka, M., Javot, H., Gout, E., Gerbeau, P., Luu, D.-T., Bligny, R., and Maurel, C. (2003). Cytosolic pH regulates root water transport during anoxic stress through gating of aquaporins. Nature *425*, 393–397.

van Dongen, J.T., Fröhlich, A., Ramírez-Aguilar, S.J., Schauer, N., Fernie, A.R., Erban, A., Kopka, J., Clark, J., Langer, A., and Geigenberger, P. (2009). Transcript and metabolite profiling of the adaptive response to mild decreases in oxygen concentration in the roots of Arabidopsis plants. Ann. Bot. (Lond.) *103*, 269–280.

Vashisht, D., Hesselink, A., Pierik, R., Ammerlaan, J.M., Bailey-Serres, J., Visser, E.J., Pedersen, O., van Zanten, M., Vreugdenhil, D., Jamar, D.C., et al. (2011). Natural variation of submergence tolerance among *Arabidopsis thaliana* accessions. New Phytol. *190*, 299–310.

Wang, M., Zheng, Q., Shen, Q., and Guo, S. (2013). The critical role of potassium in plant stress response. Int. J. Mol. Sci. *14*, 7370–7390.

Wiengweera, A., and Greenway, H. (2004). Performance of seminal and nodal roots of wheat in stagnant solution: K^+ and P uptake and effects of increasing O_2 partial pressures around the shoot on nodal root elongation. J. Exp. Bot. *55*, 2121–2129.

Zhong, S., and Chang, C. (2012). Ethylene signalling: The CTR1 protein kinase. In Annual Plant Reviews Volume 44: The Plant Hormone Ethylene, M.T. McManus, ed. (Wiley-Blackwell), pp. 147–168.

Please cite this article in press as: Shahzad et al., A Potassium-Dependent Oxygen Sensing Pathway Regulates Plant Root Hydraulics, Cell (2016), http://dx.doi.org/10.1016/j.cell.2016.08.068

STAR★METHODS

KEY RESOURCES TABLE

REAGENT or RESOURCE	SOURCE	IDENTIFIER
Antibodies		
anti-RAP2.12	Licausi et al., 2011	N/A
Anti-Rabbit IgG (whole molecule)–Peroxidase	Sigma-Aldrich	Cat#A6154; RRID:AB_258284
Chemicals, Peptides, and Recombinant Proteins		
Protease inhibitor cocktail	Sigma-Aldrich	Cat#P-8215
EASYTIDES ATP,[γ-^{32}P]	PERKIN EMER	Cat#BLU502H250UC
MAAIISDFIPPPRSRRVTSEFIWPKKK	This paper	N/A
MAAIIADFIPPPRSRRVTSEFIWPKKK	This paper	N/A
MAAIISDFIPPPRARRVTSEFIWPKKK	This paper	N/A
MAAIISDFIPPPRSRRVASEFIWPKKK	This paper	N/A
MAAIISDFIPPPRSRRVTAEFIWPKKK	This paper	N/A
MAAIIADFIPPPRARRVAAEFIWPKKK	This paper	N/A
Critical Commercial Assays		
iProof High-Fidelity PCR Kit	Bio-Rad	Cat#172-5330
Pfu DNA polymerase	Promega	Cat#M7741
RNeasy MinElute Cleanup Kit	QIAGEN	Cat#74204
DNase treatment	QIAGEN	Cat#79254
TRIzol Reagent	Invitrogen	Cat#15596026
RNA 6000 Nanochips	Agilent Technologies	Cat#5067-1511
GeneChip WT PLUS Reagent Kit	Affymetrix	Cat#902280
ARABIDOPSIS GENE1.1ST ARRAY STRIP	Affymetrix	Cat#901793
SV Total RNA Isolation System	Promega	Cat#Z3100
M-MLV Reverse Transcriptase, RNase H Minus, Point Mutant	Promega	Cat#M3681
Oligo(dT)$_{15}$ Primer	Promega	Cat#C1101
SYBR Premix Ex Taq II (Tli RNaseH Plus)	Clonetech	Cat#RR820Q
Bio-Rad protein assay	Bio-Rad	Cat#000-706
GST Sepharose 4B beads	GE Healthcare	Cat#17-0756-01
His Mag Sepharose Ni	GE Healthcare	Cat#17-3712-20
Deposited Data		
Microarray data	This paper	GEO: GSE78087
Experimental Models: Organisms/Strains		
Bur-0 x Col-0 RILs	Versailles *Arabidopsis* Stock Center	20RV
HIFs	Versailles *Arabidopsis* Stock Center	20HV289
T-DNA mutant line of *A. thaliana* (insertion in At3g24710)	NASC	N672257
T-DNA mutant line of *A. thaliana* (insertion in At3g24715) (*hcr1-1*)	NASC	N694188
T-DNA mutant line of *A. thaliana* (insertion in At3g24715) (*hcr1-2*)	NASC	N691448
T-DNA mutant line of *A. thaliana* (insertion in At3g24730)	NASC	N686911
T-DNA mutant line of *A. thaliana* (insertion in At3g24730)	NASC	N518763
T-DNA mutant line of *A. thaliana* (insertion in At3g24730)	NASC	N818835
T-DNA mutant line of *A. thaliana* (insertion in At3g24740)	NASC	N695103

(*Continued on next page*)

Continued

REAGENT or RESOURCE	SOURCE	IDENTIFIER
T-DNA mutant line of *A. thaliana* (insertion in At3g24730)	NASC	N613933
T-DNA mutant line of *A. thaliana* (insertion in At3g24730)	NASC	N807684
Aa-0 (*A. thaliana* accession)	NASC	N28007
Ag-0 (*A. thaliana* accession)	NASC	N76087
Alst-1 (*A. thaliana* accession)	NASC	N28013
Amel-1 (*A. thaliana* accession)	NASC	N28014
An-1 (*A. thaliana* accession)	NASC	N76091
Ang-0 (*A. thaliana* accession)	NASC	N28018
App1-16 (*A. thaliana* accession)	NASC	N76092
Ba-1 (*A. thaliana* accession)	NASC	N28053
Bla-1 (*A. thaliana* accession)	NASC	N76097
Boot-1 (*A. thaliana* accession)	NASC	N28091
Bor-4 (*A. thaliana* accession)	NASC	N76100
Bsch-0 (*A. thaliana* accession)	NASC	N28099
Bu-0 (*A. thaliana* accession)	NASC	N76103
Bur-0 (*A. thaliana* accession)	NASC	N76105
Col-0 (*A. thaliana* accession)	NASC	N76113
Ct-1 (*A. thaliana* accession)	NASC	N76114
Edi-0 (*A. thaliana* accession)	NASC	N76126
Est-1 (*A. thaliana* accession)	NASC	N76127
Fei-0 (*A. thaliana* accession)	NASC	N76129
Ge-0 (*A. thaliana* accession)	NASC	N76135
Gel-1 (*A. thaliana* accession)	NASC	N28279
Got-7 (*A. thaliana* accession)	NASC	N76136
Gr-1 (*A. thaliana* accession)	NASC	N76137
Gy-0 (*A. thaliana* accession)	NASC	N76139
Ha-0 (*A. thaliana* accession)	NASC	N28336
Hey-1 (*A. thaliana* accession)	NASC	N28344
Hh-0 (*A. thaliana* accession)	NASC	N28345
Hn-0 (*A. thaliana* accession)	NASC	N28350
Hod (*A. thaliana* accession)	NASC	N76141
Hov4-1 (*A. thaliana* accession)	NASC	N76142
Hovdala-2 (*A. thaliana* accession)	NASC	N76143
Hs-0 (*A. thaliana* accession)	NASC	N76145
In-0 (*A. thaliana* accession)	NASC	N76147
Jl-3 (*A. thaliana* accession)	NASC	N28369
Kelsterbach-4 (*A. thaliana* accession)	NASC	N76152
Kl-5 (*A. thaliana* accession)	NASC	N28394
Koln (*A. thaliana* accession)	NASC	N76155
Kro-0 (*A. thaliana* accession)	NASC	N28420
Ler-1 (*A. thaliana* accession)	NASC	N76164
Lom1-1 (*A. thaliana* accession)	NASC	N76174
Lp2-2 (*A. thaliana* accession)	NASC	N76176
Lp2-6 (*A. thaliana* accession)	NASC	N76177
Mt-0 (*A. thaliana* accession)	NASC	N76192
Mz-0 (*A. thaliana* accession)	NASC	N76193
N13 (*A. thaliana* accession)	NASC	N76194

(*Continued on next page*)

Continued

REAGENT or RESOURCE	SOURCE	IDENTIFIER
Nd-1 (*A. thaliana* accession)	NASC	N76197
NFA-10 (*A. thaliana* accession)	NASC	N76198
No-0 (*A. thaliana* accession)	NASC	N28564
Nw-0 (*A. thaliana* accession)	NASC	N28573
Oy-0 (*A. thaliana* accession)	NASC	N76203
Pu2-23 (*A. thaliana* accession)	NASC	N76215
Ren-1 (*A. thaliana* accession)	NASC	N76218
Rev-2 (*A. thaliana* accession)	NASC	N76219
Rsch-4 (*A. thaliana* accession)	NASC	N76222
Sanna-2 (*A. thaliana* accession)	NASC	N76223
Se-0 (*A. thaliana* accession)	NASC	N76226
Sei-0 (*A. thaliana* accession)	NASC	N28729
Sg-1 (*A. thaliana* accession)	NASC	N28732
Sp-0 (*A. thaliana* accession)	NASC	N28743
Sparta-1 (*A. thaliana* accession)	NASC	N76229
Ste-3 (*A. thaliana* accession)	NASC	N76232
T1110 (*A. thaliana* accession)	NASC	N76236
Ting-1 (*A. thaliana* accession)	NASC	N28759
Tomegap-2 (*A. thaliana* accession)	NASC	N76250
Tottarp-2 (*A. thaliana* accession)	NASC	N76251
Tsu-0 (*A. thaliana* accession)	NASC	N28780
Ty-0 (*A. thaliana* accession)	NASC	N28786
Uk-1 (*A. thaliana* accession)	NASC	N28787
Utrecht (*A. thaliana* accession)	NASC	N28795
Wei-0 (*A. thaliana* accession)	NASC	N76301
Yo-0 (*A. thaliana* accession)	NASC	N76305
Zu-1 (*A. thaliana* accession)	NASC	N28847
Recombinant DNA		
pGreen 0179; genomic HCR1-Col-0	This paper	N/A
pGreen 0179; genomic HCR1-Bur-0	This paper	N/A
pGreen 0179; genomic HCR1-Fei-0	This paper	N/A
pGreen 0179; genomic HCR1-Zu-1	This paper	N/A
pGreen 0029; promHCR1-Col-0::GUS	This paper	N/A
pGreen 0179; promHCR1::HCR1::GFP	This paper	N/A
pGreen 0179; promHCR1:: GFP::HCR1	This paper	N/A
pGWB501; d35S::HCR1-Col-0	This paper	N/A
pGEX-6P-1; GST::HCR1$_{801-1117}$ (Col-0)	This paper	N/A
pGEX-6P-1; GST::HCR1$_{801-1117}$ (Bur-0)	This paper	N/A
pGEX-6P-1; GST::HCR1$_{801-1117}$ (Fei-0)	This paper	N/A
pGEX-6P-1; GST::HCR1$_{801-1117}$ (Zu-1)	This paper	N/A
pGEX-6P-1; GST::HCR1$_{821-1117}$ (Col-0)	This paper	N/A
Software and Algorithms		
Affymetrix Expression Console software	Affymetrix	http://www.affymetrix.com/estore/browse/level_seven_software_products_only.jsp?productId=131414#1_1
Transcriptome Analysis Console v2.0 (TAC)	Affymetrix	http://www.affymetrix.com/support/learning/training_tutorials/tac_ec/index.affx

(*Continued on next page*)

Continued

REAGENT or RESOURCE	SOURCE	IDENTIFIER
Venn-diagram drawer	Bioinformatics and Evolutionary Genomics	http://bioinformatics.psb.ugent.be/webtools/Venn/
LightCycler Software	Roche Life Sciences	RRID:SCR_012155
Statistica	StatSoft	RRID:SCR_014213
Other		
See Table S7 for primer sequences	This paper	N/A
HCR1 sequences data from *Arabidopsis* accessions	The 1001 Genomes Consortium, 2016	http://signal.salk.edu/atg1001/3.0/gebrowser.php

CONTACT FOR REAGENT AND RESOURCE SHARING

Further information and requests for reagents may be directed to, and will be fulfilled by the corresponding author Christophe Maurel (christophe.maurel@supagro.inra.fr).

EXPERIMENTAL MODEL AND SUBJECT DETAILS

The *Arabidopsis thaliana* accessions Col-0 (186AV) and Bur-0 (172AV), the core population of RILs (20RV) corresponding to a F8 generation obtained by crossing these accessions, and the fixed HIF (20HV289) were obtained from the Versailles *Arabidopsis* Stock Center (Institut Jean-Pierre Bourgin, INRA, Versailles, France). For more details see http://publiclines.versailles.inra.fr/. The set of 72 *Arabidopsis* wild accessions and all T-DNA mutant lines used in this work were obtained from the Nottingham *Arabidopsis* Stock Centre (NASC) (Key Resources Table and Table S3). The T-DNA left border (LBb1.3) primer along with right primer (RP) were used for confirmation of insertion, and the left primer (LP) and RP were used to screen the homozygous plants (Table S7). For Lp_r phenotyping plants were grown in hydroponic conditions described in Method Details. Plant growth under hypoxia or normoxia refers to cultures in the absence or presence of additional air bubbling in the root bathing solution. The partial pressure for O_2 was 11.1% ± 1.1% and 20.1% ± 0.3%, respectively. For screening purposes, plants were exposed to various hormonal or abiotic stress treatments as described in Table S4.

METHOD DETAILS

Growth Conditions

Seeds were surface sterilized and sown on 0.5 × MS agar vertical plates [2.2 g L^{-1} MS (Sigma), 1% sucrose (Euromedex), 0.05% MES (Euromedex), and 0.7% agar (Sigma), pH 5.7 adjusted using KOH]. Plates were incubated for at least 2 days at 4°C in dark for stratification. Plants were germinated and further grown on these plates for 10 days in a growth chamber at 70% relative humidity (RH) and 20°C, with cycles of 16 hr of light (250 μE m^{-2} s^{-1}) and 8 hr of night. For standard conditions, seedlings were transferred to a hydroponic medium [1.25 mM KNO_3, 0.75 mM $MgSO_4$, 1.5 mM $Ca(NO_3)_2$, 0.5 mM KH_2PO_4, 50 μM Fe-EDTA, 50 μM H_3BO_3, 12 μM $MnSO_4$, 0.70 μM $CuSO_4$, 1 μM ZnSO4, 0.24 μM MoO_4Na_2, 100 μM Na_2SiO_3]. The plants were further grown for 11-13 days under the same growth conditions. The growth medium was replaced every week. Normoxic conditions were generated by bubbling air into the hydroponic medium. To study the effects of RH on Lp_r, RH in the growth chamber was increased to 90% while other growth conditions were kept constant. Plants were covered under a white nylon sheet to explore effects of irradiance on Lp_r. Medium compositions for investigating the effects of different nutrients or hormones on Lp_r are presented in Table S4. For flooding assays, 10-day-old seedlings were waterlogged or submerged in 0.1% agar 0.5 × MS medium for 3 hr or 4 days, respectively. Shoots were harvested immediately after waterlogging. For submergence assays, the plants were transferred back to 0.7% agar 0.5 × MS plates, and shoots were harvested after 4 days of recovery. For submergence experiments in soil grown plants, seeds were germinated on 0.5 × MS agar medium for 2 weeks in a growth chamber at 65% RH and 20°C, with cycles of 8 hr of light (250 μE m^{-2} s^{-1}) and 16 hr of night, transferred to soil and grown for 3 more weeks. Then, plants were submerged in water for 4 days. Shoots were harvested after 8 days of recovery.

Plant Phenotyping for Water Relations

For measurement of Lp_r, a freshly detopped *Arabidopsis* root system was inserted into a pressure chamber filled with hydroponic medium at a pH adjusted to 6.5 using KOH, or NaOH for K^+ starved roots. The hypocotyl was tightly sealed inside a combination of plastic and metallic seals using a low-viscosity dental paste (President Light, Coltene, Switzerland). The rate of pressure (*P*)-induced sap flow (*Jv*) exuded from the hypocotyl section was recorded using high-accuracy flow meters (Bronkhorst, France) in an automated manner using a LabVIEW-derived application. In practice, excised roots were subjected to a pretreatment at

350 kPa for 10 min to attain flow equilibration, and *Jv* was measured successively at 320, 160, and 240 kPa for about 2 min. Root dry weight (DW_r) was measured after measurement of *Jv*. The Lp_r (ml g^{-1} hr^{-1} MPa^{-1}) of an individual root system was calculated using the following equation:

$$Lp_r = Jv/(DW_r \cdot P)$$

In NaN_3 and mercury inhibition experiments, Lp_r was derived from continuous *Jv* measurement at 320 kPa as described (Sutka et al., 2011). Shoot water contents were determined as described (Koffler et al., 2014).

QTL and Fine Mapping

For QTL mapping, plants were grown under hydroponic conditions without air bubbling to achieve homogeneous plant growth. The phenotypic data for root hydraulics [conductivity (Lp_r) and conductance (L_0)] and plant growth [shoot dry weight (DWs), DWr, and DWs/DWr] were obtained from a sub-set of 123 Bur-0 × Col-0 RILs from the core population. The phenotypic values are the mean of 7-8 plants per RIL. Multiple QTL mapping (MQM) was performed on traits using R/qtl (Arends et al., 2014). Missing genotype data were filled in using augmentation function. Three markers were chosen as cofactors for unsupervised backward elimination.

For confirmation of the Lprm320 QTL, fixed HIFs were generated using the segregating F7 RIL 20RV289. Two derived lines that differ only for the allele present at the region of interest (HIF289-Bur-0 and HIF289-Col-0) were further characterized. A fine-mapping population was developed by self-fertilization of an HIF289 individual that was still heterozygous for the QTL region, and a total of 80 individuals recombined within the candidate interval (rHIF) were identified. They were further genotyped with additional markers to locate the recombination breakpoint (primer sequences provided in Table S7) between MSAT3.06375 and MSAT3.23 markers (Figure S1A). rHIFs showing recombination at different intervals were phenotypically tested through their segregating descendants in a "progeny testing" process to see if genotypic segregation was linked with segregation of Lp_r phenotype.

Quantitative and Molecular Complementation

The advanced rHIFs (arHIFs) were developed by crossing two close rHIFs (rHIF289-53 and rHIF289-57) contrasted for the QTL segregation but not the surrounding region to generate a near-isogenic line segregating for a small interval of 15kb. For quantitative complementation, plants carrying one of the two allelic forms, arHIF289-Col-0 or arHIF289-Bur-0, were selected and used for making independent reciprocal crosses with *hcr1-2* [N691448 (SALK_203216C); T-DNA insertion on Chr3: 9029466-9029674] and Col-0 plants. F1 plants were phenotyped for Lp_r, and each individual plant was genotyped using the marker IND3.07395 to ensure that it was a real F1 with the expected allelic combination at Lprm320. For molecular complementation, a 6038 bp genomic region (Chr3: 9024368-9030405, corresponding to Col-0 TAIR10 sequence) harboring *HCR1* was PCR amplified from Bur-0, Col-0, Fei-0, or Zu-1 genomic DNA using iProof High-Fidelity PCR Kit (Bio-Rad). The amplicons were cloned in a plant expression vector (pGreen 0179). For constitutive overexpression of HCR1, the coding sequence of HCR1 was amplified from Col-0 cDNA and cloned in a pGWB501 vector under the control of d35S promoter. The recombinant vectors were used for transformation of *hcr1-1* plants [N694188 (SALK_205151C); T-DNA insertion on Chr3: 9027411-9027663] using the floral dip method. Homozygous transformants in T2 generation were selected on hygromycin B (30 mg L^{-1}), and 2-5 independent lines were phenotyped for Lp_r.

Microarray Analysis

Arabidopsis Col-0 and *hcr1* plants were grown under hypoxia in the presence of K^+, and root samples of 21-day-old plants were harvested. Each sample was a pool of five plants, and each type of sample was harvested in triplicate. Total RNAs were isolated using TRIzol reagent (Invitrogen) and purified using the RNeasy MinElute Cleanup Kit (QIAGEN) after DNase treatment (QIAGEN). RNA quantities were assessed with a NanoDrop ND-1000 spectrophotometer (Thermo Fischer Scientific) and RNA qualities using RNA 6000 Nanochips with a 2100 Bioanalyzer (Agilent). For each sample, 100 ng of total RNA were amplified using the GeneChip WT PLUS Reagent Kit (Affymetrix) following the manufacturer's instructions. Ten μg of the resulting biotin-labeled single stranded cDNA were used for hybridization to *ARABIDOPSIS* GENE1.1ST ARRAY STRIP (Affymetrix). Hybridization was carried out at 45°C for 16 hr, and the arrays were washed and stained according to the protocol described in the Manual Target Preparation for GeneChip Whole Transcript (WT) Expression Arrays (Affymetrix). The arrays were scanned using a GeneAtlas Imaging Station (Affymetrix). The quality of hybridization was evaluated using the Expression Console software (Affymetrix). Normalized expression signals were calculated from Affymetrix CEL files using the Robust Multi-Array average normalization method. Differentially expressed genes (ANOVA $p < 0.05$ and ≥ 1.5-fold change) in either of *hcr1* mutant line compared to Col-0 were identified using the Transcriptome Analysis Console v2.0 software (Affymetrix). Venn-diagram was drawn using the web based server Bioinformatics and Evolutionary Genomics (http://bioinformatics.psb.ugent.be/webtools/Venn/).

Quantitative Real Time-PCR

Col-0 and *hcr1* plants were grown under hypoxia or normoxia in the presence or absence of K^+. Total RNAs were isolated from roots using a SV Total RNA Isolation System (Promega) following the manufacturer's instructions. Four μg of total RNA were used as a template for first strand cDNA synthesis, which was performed using M-MLV Reverse Transcriptase, RNase H Minus, Point Mutant (Promega) and $Oligo(dT)_{15}$ Primer (Promega) in a final volume of 40 μl, according to the instructions from the manufacturer. First

strand cDNA was diluted 4 times. Twenty five ng of first strand cDNA were used as template for qRT-PCRs which were performed in 384-well plates with a LightCycler 480 Real-Time PCR System (Roche diagnostics). SYBR Green was used to monitor cDNA amplification at an annealing temperature of 57°C. Primer efficiencies for each pair were evaluated from the analysis of 1:4, 1:16 and 1:64 dilutions of first strand cDNA. *UBQ10* [At4g05320] and/or *F-box* family protein [At5g15710] were used as internal controls. The primer sequences used are described in Table S7.

GUS Assays

HCR1 putative promoter (1481 bp) was PCR amplified from genomic DNA of Col-0 using iProof High-Fidelity PCR Kit (Bio-Rad). The primer sequences are provided in Table S7. The PCR product was cloned in a modified pGreen 0029 vector, upstream of a GUS coding DNA sequence. The recombined vector was used for transforming Col-0 plants as described above, and the T2 homozygous transformants were selected on kanamycin (50 mg L^{-1}). Three independent homozygous T2 lines were used for histochemical GUS staining. Plants for GUS staining in vegetative tissues were grown under K^+-replete hypoxia, and in soil for assays in reproductive tissues.

Western Hybridization

Col-0 and *hcr1* plants were cultured under K^+-replete O_2-deficient hydroponic conditions. Five independent experiments were performed while analyzing pool of 4-5 plant roots during each experiment. Total proteins were extracted using trichloricacetic acid/acetone from roots. Detection of RAP2.12 was performed through western hybridization using an anti-RAP2.12 antibody as described previously (Licausi et al., 2011). Quantification of RAP2.12 corresponding bands was performed using an ImageJ program (NIH, USA).

Sub-cellular Localization of HCR1

For sub-cellular localization studies, green fluorescent protein (GFP) was fused to either C- or N terminus of Col-0 HCR1 coding sequence under the control of the *HCR1* putative promoter and terminator regions. For this purpose, Splicing by Overlap Extension (SOEing) PCR protocol was used to join the four DNA molecules in each case (see Table S7 for primer sequences). All the PCRs were performed using iProof High-Fidelity PCR Kit (Bio-Rad). The resulting recombined DNA molecules were cloned in pGreen 0179. *hcr1-1* mutant plants were transformed as described above, and homozygous plants in T2 generation were selected on hygromycin B (30 mg L^{-1}). Two to 3 independent transgenic lines for GFP fusions with HCR1 were observed using a confocal laser-scanning microscope (Zeiss LSM510 AX70). To further clarify the nuclear localization of HCR1, we used DAPI staining as it is documented to stain DNAs but is excluded from the nucleolus. Quantification of mean gray values was performed using a ImageJ program (NIH, USA).

pH Measurements

Fluorescein was used for quantifying proton concentrations due to its pH-dependent excitation spectrum. In practice, roots of plants grown in hydroponics for 3-4 weeks were incubated with 2 μM fluorescein diacetate for 10 min and washed twice in growing medium. Samples were illuminated at two excitation wavelengths, 438/24 nm and 475/28 nm and fluorescence light was collected with a 525/45 BP filter. To convert ratio to pH values, a calibration curve was made by incubating fluorescein with 50 mM Mes-KOH or HEPES-KOH solutions at different pH.

Protein Purification and Kinase Assays

The HCR1 putative kinase domain (Met821-Pro1117) or a longer fragment of HCR1 (Glu801-Pro1117) were amplified by PCR from cDNA of Col-0, Bur-0, Fei-0 or Zu-1 using *Pfu* DNA polymerase (Promega). The sequences of primers are listed in Table S7. The amplicons were cloned into a pGEX-6P-1 expression vector (GE Healthcare). For protein expression, BL21 Rosetta bacteria were transformed with recombinant pGEX-6P-HCR1. Protein production was induced with 0.1 mM IPTG for 3 hr at 28°C. Bacteria were then collected by centrifugation (5000 rpm, 15 min). The cell pellet was lysed for 30 min on ice in 2 ml per 50 ml culture volume of lysis buffer [250 mM NaCl, 1% Triton X-100, 5 mM DTT, 10% glycerol, 1 mg mL^{-1} lysozyme, protease inhibitor cocktail (Sigma), 50 mM Tris-HCl, pH 7.5]. Lysate was then snap-frozen in liquid nitrogen and rapidly de-frozen at 42°C for 4 times before centrifugation (13 000 rpm, 15 min). Recombinant glutathione-S-transferase (*GST*)::HCR1 was purified in batch with Glutathione Sepharose 4B beads (GE Healthcare). Soluble protein fraction was added to Glutathione Sepharose beads and the slurry was gently shaken for 3 hr or overnight at 4°C. The beads were washed 3 times with PBS, centrifuged at 1000 × *g* for 5 min. The fused protein was eluted in 200 mM NaCl, 20 mM reduced glutathione, 50 mM Tris-HCl, pH 8.0. Protein was concentrated on an Amicon Ultra-15 30K filtration unit (Millipore) and supplemented with 30% glycerol before storage at −50°C. Protein concentration was determined by a Bradford protein assay.

The RAP2.12 coding sequence was PCR amplified from Col-0 cDNA using a iProof High-Fidelity PCR Kit (Bio-Rad). The primer sequences used for PCR are provided in Table S7. The PCR product was cloned in a pIVEX WG His-6 tag vector (5PRIME). RAP2.12 protein was produced in vitro using a RTS 100 Wheat Germ CEFC Kit (5PRIME) following manufacturer's instructions. The protein was purified using His Mag Sepharose Ni magnetic beads (GE Healthcare) using 5 mM imadizole, 500 mM NaCl, 20 mM Na_2PO_4, 8 M urea for binding/washing and 250 mM imadizole, 500 mM NaCl, 20 mM Na_2PO_4, 8 M urea for elution.

HCR1 kinase activity was determined in a solution containing 50 mM KCl, 10 mM $MgCl_2$, 5 mM $MnCl_2$, 25 mM glycerophosphate, 1 mM DTT, 50 mM HEPES pH 7.5, 500 ng HCR1 kinase domain, 1 μg MBP or 200 μM of the indicated RAP2.12 peptide, 100 μM [γ-^{32}P]ATP (200 Ci mol^{-1}). RAP2.12 N terminus peptide sequences were as follows:

pep27: MAAIISDFIPPPRSRRVTSEFIWPKKK,
pep27S8A: MAAIIADFIPPPRSRRVTSEFIWPKKK,
pep27S16A: MAAIISDFIPPPRARRVTSEFIWPKKK,
pep27T20A: MAAIISDFIPPPRSRRVASEFIWPKKK,
pep27S21A: MAAIISDFIPPPRSRRVTAEFIWPKKK,
pep27STallA: MAAIIADFIPPPRARRVAAEFIWPKKK.

Reactions were carried out in 50 μl for 45 min at room temperature. They were either stopped with a Laemmli buffer and separated by 12% SDS-PAGE or spotted on phosphocellulose paper P81 (Reaction Biology Corp.). Gels were fixed in 50% methanol, 10% acetic acid, Coomassie blue stained and dried in ethanol before exposition in a FLA-5000 Fluorescent Radioactive Image Analyzer (Fujifilm). Phosphocellulose papers were washed for 3 × 5 min in 75 mM phosphoric acid and once with acetone and radioactivity was determined on a TRI-CARB Phosphor Imager (Packard). RAP2.12 full-length protein phosphorylation by HCR1 was studied by means of a modified far western protocol, using RAP2.12 as prey and HCR1 as bait in the presence of radiolabeled ATP. Briefly, purified RAP2.12 or MBP were separated by gel electrophoresis and blotted onto PVDF membranes (Millipore). The latter were blocked for 1 hr in PBS with 1% Tween and 1% BSA, and pre-incubated for 30 min in a kinase buffer (50 mM NaCl, 40 mM KCl, 10 mM $MgCl_2$, 25 mM β−glycerophosphate, 1 mM DTT, 50 mM HEPES, pH 7.5), prior to incubation for 2 hr in the presence of 50 μM ATP, 10 μCi [γ-^{32}P]ATP, and 8μg of Col-0 HRCI kinase domain (821-1117). Membranes were washed in several successive baths of TBS with 1% Tween and 0.1% TCA for 1 hr before exposition in a FLA-5000 Fluorescent Radioactive Image Analyzer (Fujifilm).

Determination of Cation Accumulation

For determination of accumulation of cations, Col-0 and *hcr1* mutant plants were grown under K^+-replete hypoxia. In order to drain off apoplastic ions, roots of 21-day-old plants were washed in a solution containing 15 mM EDTA and 2 mM $CaSO_4$ for 5 min and then in Milli-Q water for 5 min. Root samples were harvested, each sample being a pool of 4-5 plants, and each type of sample was analyzed in octuplicate coming from 4 independent experiments. The samples were dried in an air incubator at 60°C for more than 96 hr, and the dry weights were measured. To extract the minerals, tissues were digested with 1 ml of 48.75% HNO_3 and 7.5% H_2O_2 in a quartz tube at 110°C in a heat block for 2 hr. The volume of the digest was adjusted to 5 ml using Milli-Q water. An atomic absorption spectrophotometer (SpectrAA 220, Varian) was used for quantification of different cations in the extract.

QUANTIFICATION AND STATISTICAL ANALYSIS

Statistical significance of the data otherwise stated was assessed using either Student's *t* test which is represented by * at $p < 0.05$ or one-way ANOVA being represented using letters at $p < 0.05$. In figure legends n means number of plants/samples and N indicates the number of independent experiments (plant cultures). Statistical analysis were performed using *Statistica* (StatSoft). Quantitaitve data are represented as means ± SE.

DATA AND SOFTWARE AVAILABILITY

Data Resource

The accession number for the microarray data reported in this paper is GEO: GSE78087.

Cell

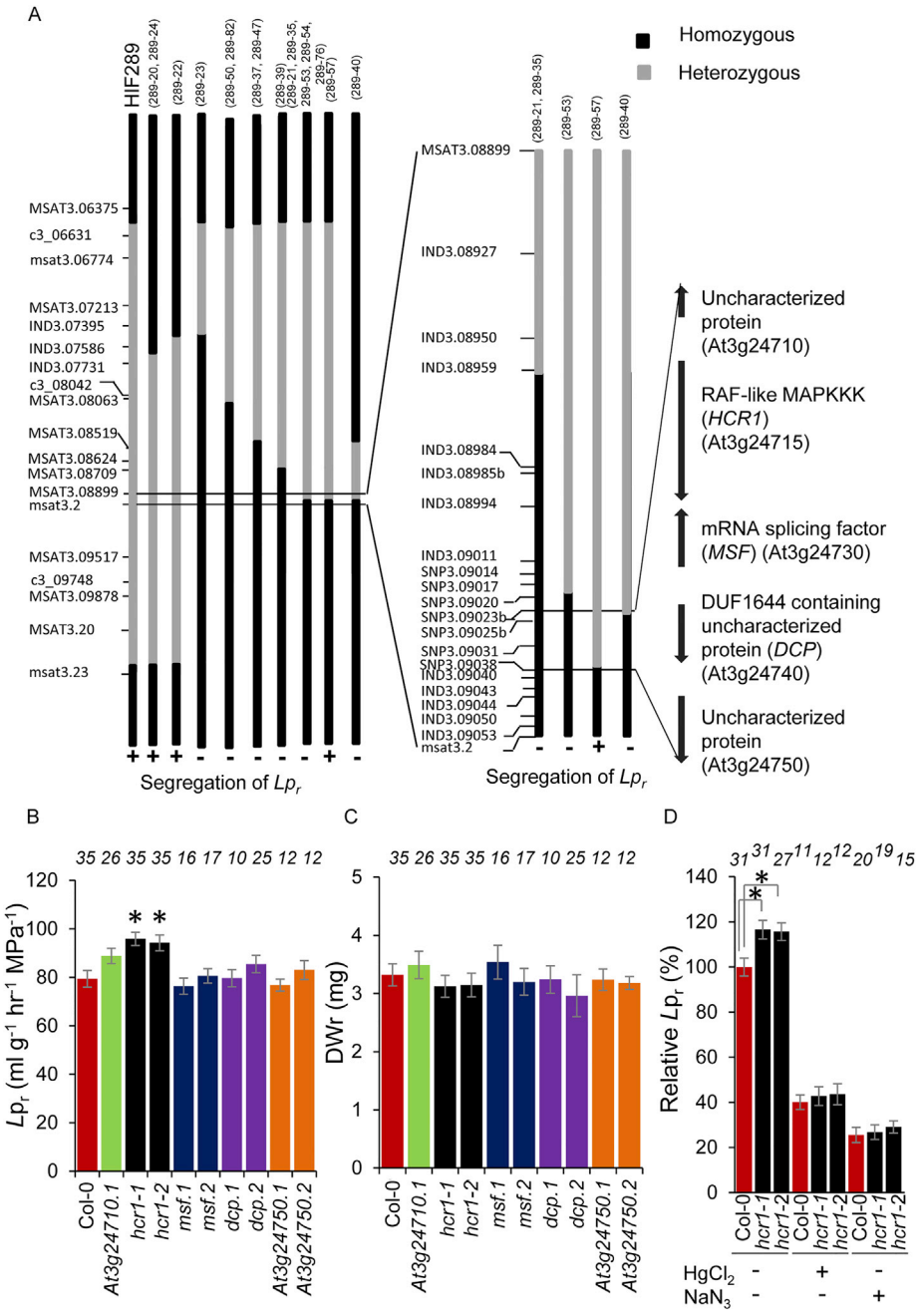

Figure S1. Positional Cloning of *HCR1*, Related to Figure 1

(A) Fine map of Lprm320 using recombinant heterogeneous inbred families (rHIFs). The genetic markers listed on the left of the map were used to restrain the QTL interval. Heterozygous and homozygous genomic regions are represented by gray and black bars, respectively. Phenotypic results for segregation (+) or lack of segregation (-) of root hydraulic conductivity (Lp_r) are indicated for each rHIF. The enlarged genomic region comprised between msat3.2 and MSAT3.08899 shows the fine mapped candidate interval revealed by differential Lp_r segregation of rHIFs 289-57 and 289-40. The genes annotated in this interval are shown.
(B and C) Lp_r (B) and root dry weight (DW_r) (C) of knockout mutants for the five candidate genes located in the Lprm320 fine mapped interval. The graphs show, for each plant line, average values ± SE from measurements on the indicated number of plants (top), with three independent plant cultures.
(D) Comparison of Col-0 and *hcr1* plants for Lp_r, before and after treatment with $HgCl_2$ or NaN_3. The graph shows average Lp_r (±SE) of each line from the indicated number of plants in two to four independent plant cultures.

Comment citer ce document :
Shahzad, Z., Canut, M., Tournaire-Roux, C., Martiniere, A., Boursiac, Y., Loudet, O., Maurel, C. (Auteur de correspondance) (2016). A potassium-dependent oxygen sensing pathway regulates plant root hydraulics. Cell, 167 (1), 87-98.e14. DOI : 10.1016/j.cell.2016.08.068

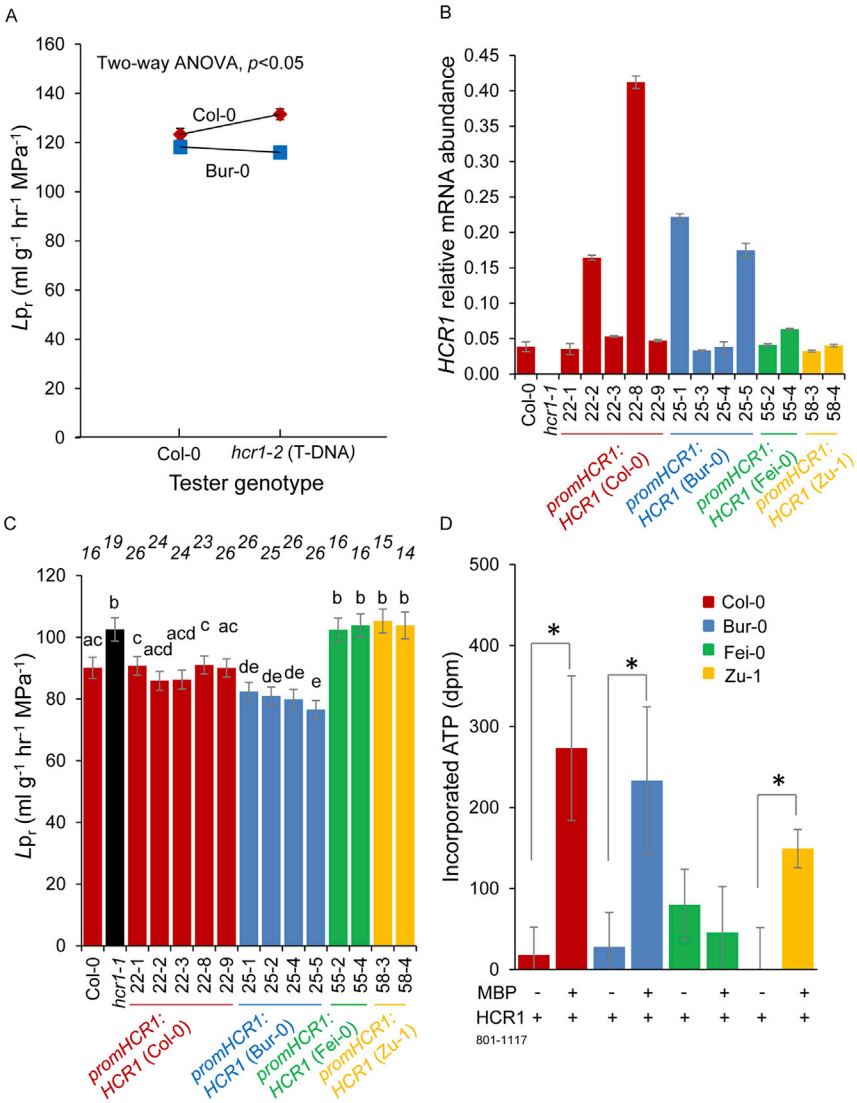

Figure S2. Quantitative and Molecular Complementation of Lprm320 and Protein Kinase Activity of HCR1 Allelic Forms, Related to Figure 1

(A) Quantitative complementation of Lprm320. Different F1 allelic combinations were obtained after crosses of either arHIF289-Col-0 or arHIF289-Bur-0 with *hcr1-2* or Col-0. Corresponding mean Lp_r ± SE values (n = 65-94, N = 3) are shown. The Lprm320 × *HCR1* genotype interaction term is significant at $p < 0.05$ (Two-way ANOVA).

(B) Transcript abundance of *HCR1* in Col-0, *hcr1-1*, and *hcr1-1* homozygous transgenic lines expressing Col-0, Bur-0, Fei-0, or Zu-1 genomic fragments containing *HCR1*. qRT-PCR was used to determine the mRNA abundance of *HCR1* relative to *UBQ10*. Data (means ± SE) from 3 independent plant cultures, each with pool of 4-5 plants per genotype.

(C) Molecular complementation of Lprm320. Lp_r was measured in the same plant lines as in (B). Average values (±SE) from 3 experiments are indicated. The number of plants phenotyped for each genotype is indicated on top. The Lp_r data from all independent transgenic lines shown for each allele in this figure were pooled and are represented in Figure 1C.

(D) In vitro kinase activity of HCR1 allelic forms. Recombinant HCR1 fragments ($HCR1_{801-1117}$) from Col-0, Bur-0, Fei-0 and Zu-1 were tested for their ability to phosphorylate MBP. For each form, $HCR1_{801-1117}$ alone was used as negative control. Means (±SE) of incorporated ATP in MBP is shown (n = 6-10, N = 3-5).

Comment citer ce document :
Shahzad, Z., Canut, M., Tournaire-Roux, C., Martiniere, A., Boursiac, Y., Loudet, O., Maurel, C. (Auteur de correspondance) (2016). A potassium-dependent oxygen sensing pathway regulates plant root hydraulics. Cell, 167 (1), 87-98.e14. DOI : 10.1016/j.cell.2016.08.068

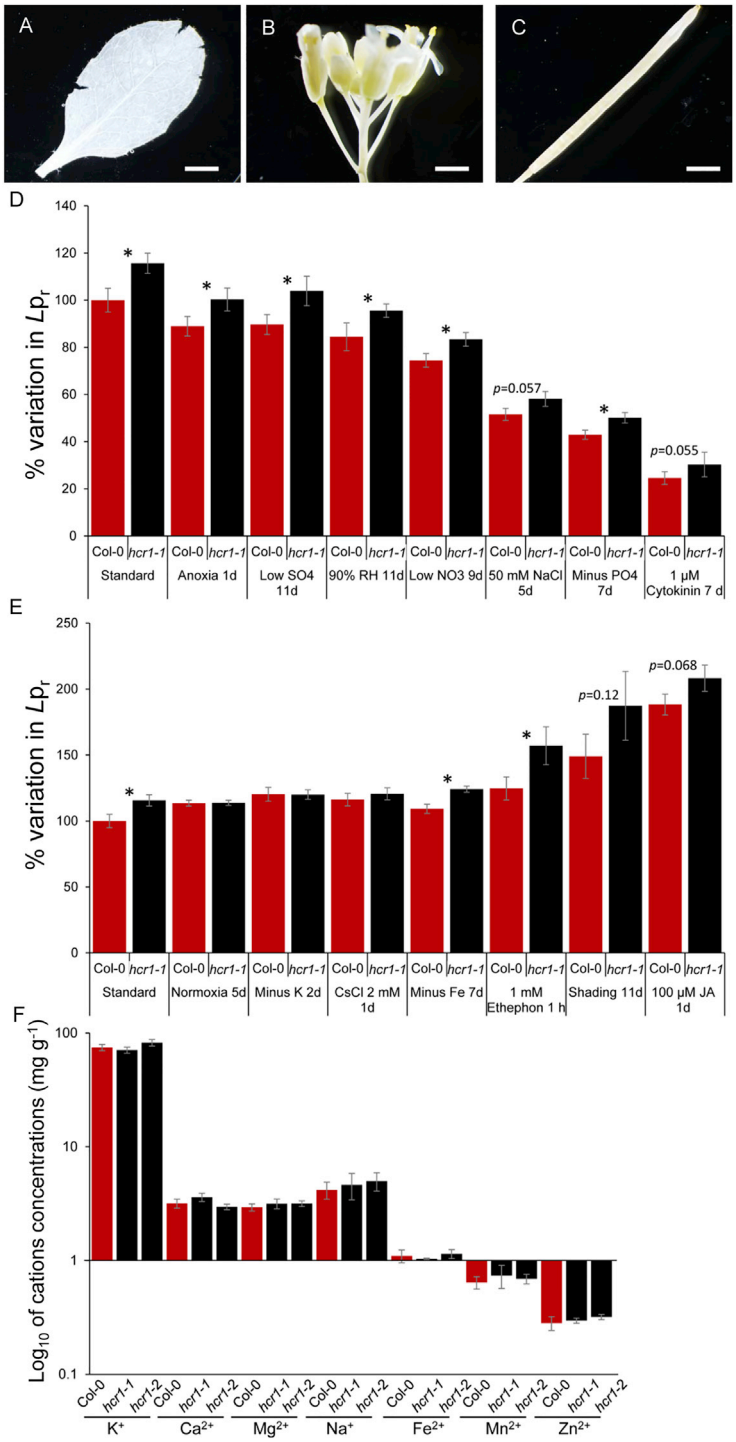

Figure S3. Tissue Localization of *HCR1* Putative Promoter Activity and Phenotypes of a *hcr1* Knockout Mutant under Various Plant Growth Conditions, Related to Figure 2

(A–C) prom*HCR1*::GUS expression was not detected in young leaves (A), inflorescences (B), or siliques (C). Scale bars: 0.5 mm

(D and E) Mean Lp_r (± SE) of Col-0 and *hcr1-1* plants grown under conditions known to influence Lp_r of Col-0 either negatively (D) or positively (E). See Table S4 for composition of modified hydroponic solutions used during this analysis. Anoxia was induced by bubbling gaseous N_2 in the root bathing solution.

(F) Mean concentration (± SE) of indicated cations in the roots of Col-0 and *hcr1* plants grown under standard conditions (n = 8, N = 4).

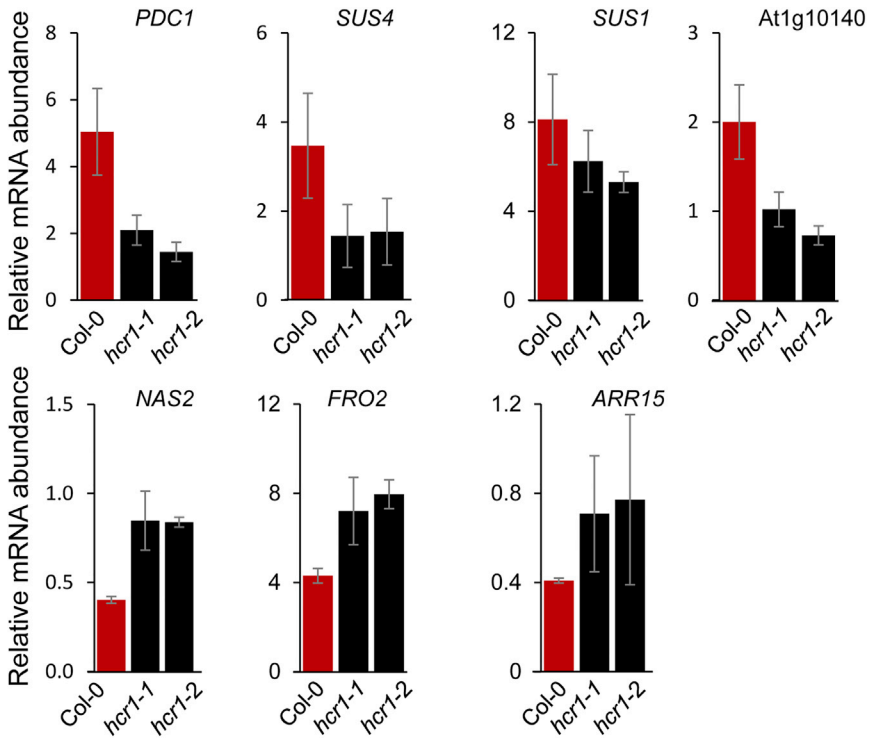

Figure S4. mRNA Abundance of Representative Hypoxia-Responsive Genes in *hcr1*, Related to Figure 3

Microarray experiments showed the indicated genes to be de-regulated in *hcr1*. Their mRNA abundance was analyzed by qRT-PCR using gene specific primer pairs (Table S7). Mean transcript levels (±SE) of each gene were determined relative to the average of *UBQ10* and *F-box* family protein mRNA levels. Data from N = 3 independent plant cultures, each with pools of 4-5 plants per genotype.

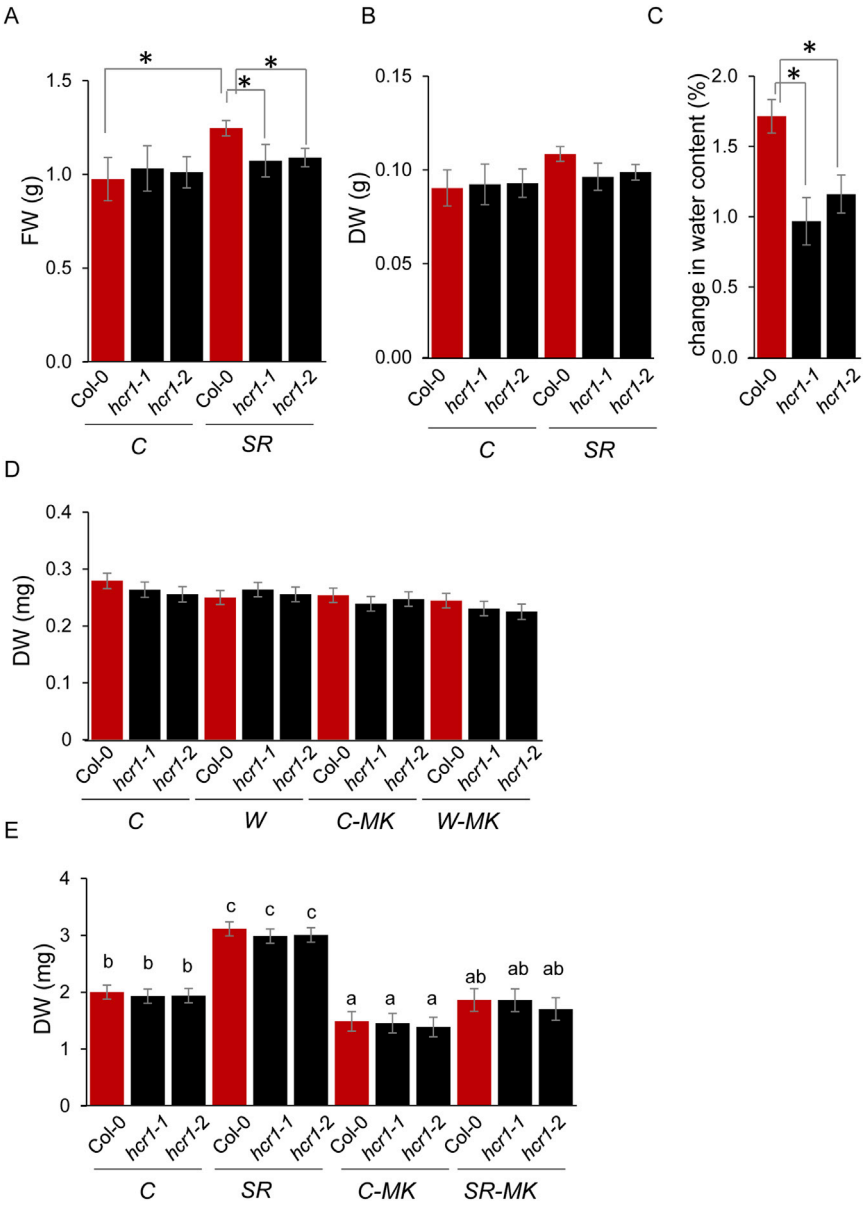

Figure S5. *HCR1* Controls Shoot Water Relations and Growth under Hypoxia, Related to Figure 5

(A–C) Shoot water relations during recovery from submergence in plants grown in soil. Five-week-old Col-0 and *hcr1* plants were submerged in water or kept under aerated conditions for 4 days under light. Plants were then transferred to aerated conditions for 8 days and their fresh weight (A), dry weight (B), and change in water content (C) were determined. Similar to Figure 5, change in water content was calculated for each genotype by reference to the corresponding control conditions (means ± SE, n = 8-10, N = 2).

(D) Mean shoot dry weight (±SE) of Col-0 and *hcr1* plants subjected to waterlogging in vitro, in the presence or absence of K^+. Data from two independent plant cultures with n = 16-19 plants per condition (*C* = control, *W* = waterlogging, *C-MK* = control without K^+, and *W-MK* = waterlogging without K^+).

(E) Effect of submergence, in the presence or absence of K^+, on mean shoot dry weight (± SE) of Col-0 and *hcr1* plants grown in vitro (n = 9-22, N = 2) (*SR* = recovery from submergence, *SR-MK* = recovery from submergence in the absence of K^+).

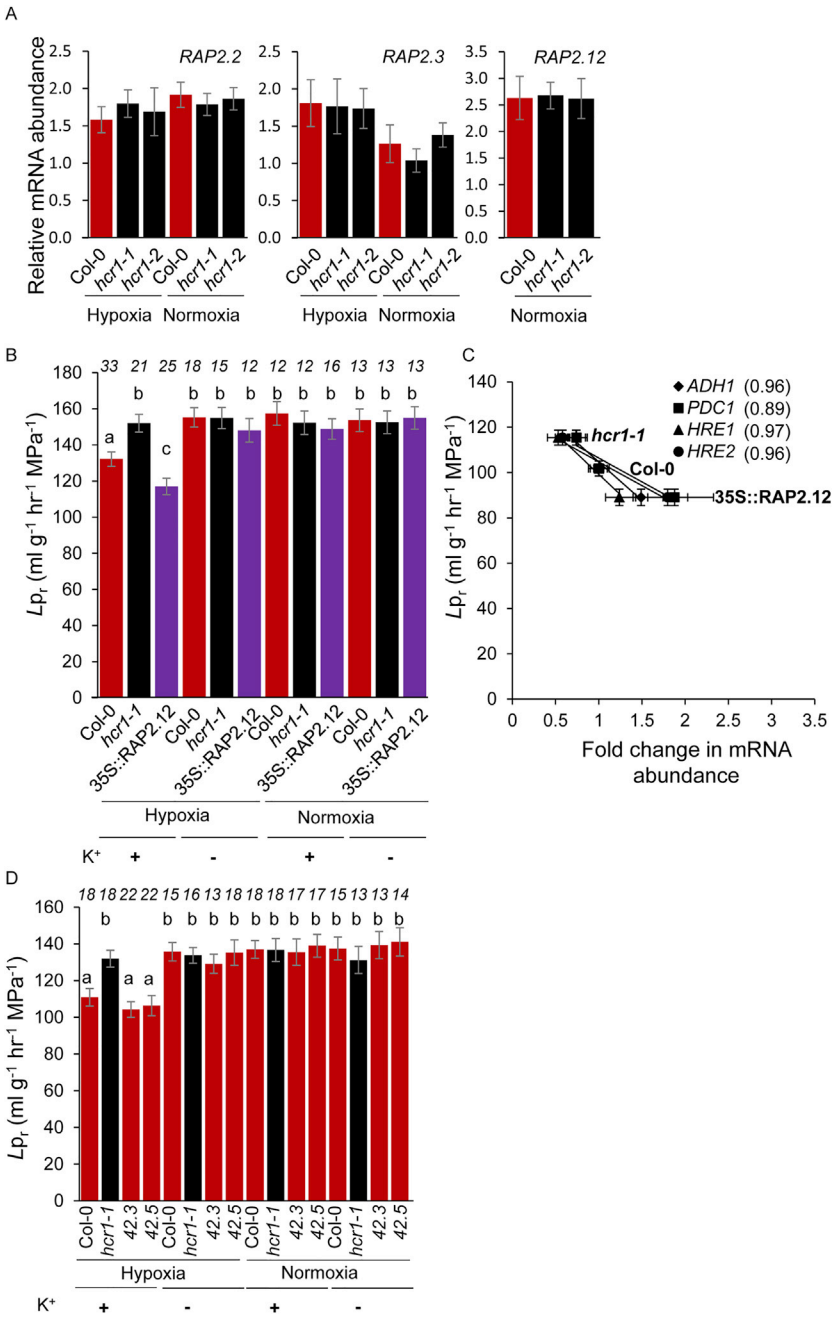

Figure S6. *HCR1* and *RAP2.12* Act in a Same Signaling Pathway, Related to Figure 6

(A) mRNA abundance of *RAP2.2*, *RAP2.3* and *RAP2.12* in the roots of Col-0 and *hcr1* plants grown under K^+-sufficient hypoxic or normoxic conditions. Mean transcript levels (±SE) were expressed relative to the average transcript levels of *UBQ10* and *F-box* family protein (n = 6, N = 3).

(B) Lp_r of Col-0, *hcr1,* and 35S::RAP2.12 plants grown under hypoxic or normoxic conditions in the presence or absence of K^+. The graph shows average Lp_r (±SE) from the indicated number of plants and three independent experiments.

(C) Correlation between Lp_r (mean ± SE) and mRNA abundance of *ADH1*, *PDC1*, *HRE1*, and *HRE2* (mean ± SE) in the roots of Col-0, *hcr1*, and 35S::RAP2.12 plants grown under K^+-replete hypoxic conditions. Transcript levels of HRGs were normalized to the average transcript levels of *UBQ10* and *F-box* family protein and represented as fold change with respect to Col-0 (n = 6, N = 3). R^2 values are shown in brackets.

(D) Average *L*pr (±SE) of Col-0, *hcr1,* and d35S::HCR1-Col-0 (transgenic lines *42.3* and *42.5*) plants grown under hypoxic or normoxic conditions in the presence or absence of K^+. Data from the indicated number of plants in three independent experiments.

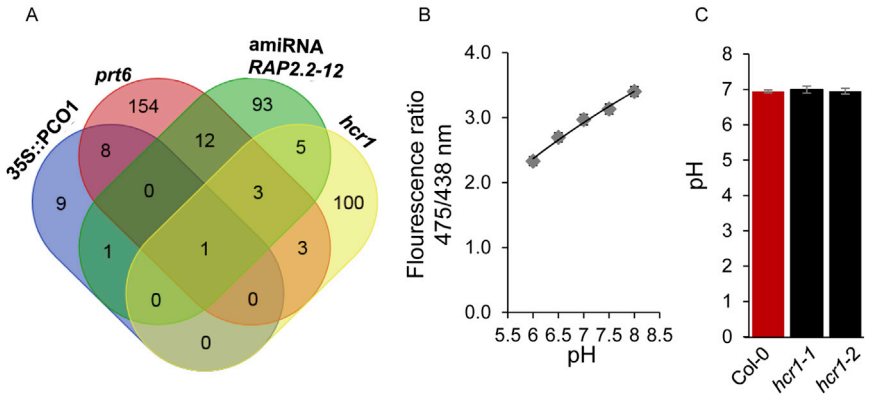

Figure S7. *HCR1* Acts on Transcriptome but Not Cytosolic pH, Related to Figure 7

(A) Venn-diagram showing overlap of deregulated transcriptome between *hcr1* and genotypes showing altered regulation of HRGs. Transcriptome comparisons were performed with respect to Col-0, under normoxic (35S::PCO1 and *prt6* (components of N-end rule pathway)) or hypoxic (*hcr1* and amiRNA line showing reduced *RAP2.2* and *2.12* expression) conditions. Transcriptomic data for genotypes other than *hcr1* were exported from Gene Expression Omnibus (GEO): GSE44344, GSE29941, and GSE29187. Transcripts showing > 1.5-fold change were considered for the analysis.

(B and C) Cytosolic pH of Col-0 and *hcr1* plants grown under hypoxia. pH measurements were made using a fluorescein-based ratiometric method. Standard curve (B) shows the relationship between the fluorescence ratio (475/438 nm) and pH. Mean cytosolic pH (±SE) measured in root cells of Col-0 and *hcr1* is shown ($n \geq 33$) (C).